An Experimental Study of the Effect of Bone Inorganic-Organic Composition on the Mechanical Properties

By

Ogheneriobororue Avwerosuo Amromanoh

A thesis submitted to the Faculty of Graduate Studies of
The University of Manitoba
In partial fulfilment of the requirements for the degree of

MASTER OF SCIENCE

Department of Mechanical Engineering
Price Faculty of Engineering
University of Manitoba
Winnipeg, Manitoba

April 2020

Abstract

Bone is a living composite material consisting of inorganic minerals, organic proteins, and water, which approximately account for 60%, 30% and 10% of bone mass, respectively. In the reported experimental studies on bone mechanical properties, attention has been focused on the effect of inorganic minerals while the role of organic proteins and water has been ignored. This neglect may explain why the existing bone mechanical models are not accurate. Furthermore, a reliable experimental protocol for the study of bone compositions and their effects on mechanical properties has not yet been established. In this thesis, the combined effect of organic proteins and water was studied by developing a novel experimental protocol. First, to reduce the effect of bone anisotropy, a unique technique was designed for the fabrication of bone specimens; Second, for the analysis of bone inorganic and organic compositions, a new ashing procedure was developed; Third, the effects of bone inorganic and organic contents on bone mechanical properties were studied by statistical analyses. The obtained results showed that there is a close correlation between bone organic content and bone stiffness.

Acknowledgments

Dedication

To my Parents.

Contents

List of Tables

List of Figures

List of Copyrighted Material

No copyrighted material was used.

List of Abbreviations

b1	Exponent number
BV	Bone Volume
CI	Confidence Interval
E	Young's Modulus
l	Length
m	Mass
M	Mean
MPa	Mega Pascals
n	Sample Size
p	Probability of statistical significance
r	Radius
R	Coefficient of Correlation
R^2	Coefficient of Determination
SD	Standard Deviation
SE	Standard Error of the Mean
TV	Total Volume
Y^{Energy}	Energy to yield

List of Symbols

ρ_{app}	Apparent Density
ρ_{ash}	Ash Density
σ^{break}	Break Stress
ρ	Density
ρ_{rat}	Density ratio
Ø	Diameter
ρ_{org}	Organic Density
σ^{peak}	Peak Stress
α	Significance level
ε	Strain Rate
σ^{yield}	Yield Stress

List of Appendices

Chapter 1

Introduction

1.1   Motivation

Osteoporosis is a degenerative bone disease characterized by bone mass loss, which makes bones susceptible to fracture [1]. Osteoporotic fracture occurs most frequently at the hips, spine, and forearm and results in adverse outcomes such as disability and even mortality [2]. Based on the increase in global life expectancy, previous studies have estimated that hip fractures would increase from 1.3 million in the year 1990 to 21.3 million by 2050 [1,3–5]. Such a dramatic increase would place a more significant burden on the healthcare system. The National Hospital Discharge Survey [6] reported that the number of hip replacements performed in the United States (on people aged 45 and over) between 2000 and 2010 increased from 138,000 to 310,000. These statistics mean that although technological advancements have increased life expectancy, the older population has an increased chance of bone-related health problems [7,8]. Increased incidences of hip fractures have, therefore, been linked with greater life spans and higher fall rates [9-11]. It is therefore critical to take

measures to combat hip fractures and alleviate the burden on the healthcare system. A deeper understanding of these fracture mechanisms would aid clinicians in reducing mortality related to hip fractures. The study of bone mechanical properties would, therefore, be necessary for the understanding of these fracture mechanisms.

Osteoporosis directly affects the functionality of the bone. Researchers have thus sought to understand the mechanism of bone strength in order to provide a solid knowledge base to combat osteoporosis. They aim to provide working solutions for managing bone health problems through various bone-testing techniques. The gold standard for testing bones and estimating their corresponding mechanical properties is direct functional mechanical tests [12]. These mechanical properties depend on the subject, composition (inclusive of biological processes), anatomic site, age and structure [13,14]. Researchers, therefore, conduct bone testing experiments with the inclusion of different combinations of those dependent factors [14].

Existing research examines the dependence of mechanical properties of bone on bone mineral density. However, bones are mainly composed of mineral content (65% by weight), organic content (35%), and water (10%). While mineral content affects the stiffness of the bone, organic content affects flexibility and ductility. The optimal combination of the mineral and organic components of the bone gives rise to its strength. This suggests that research on bone mechanical properties should examine the organic component contribution as well. Carefully designed experimental protocols that incorporate the organic component information would, therefore, need to be utilized.

Most existing experimental protocols focus on examining the dependence of mechanical properties on bone mineral density. While multiple works studying bone mechanical

properties exist, significant inter-study variations in experimental techniques are present [15]. The inter-study variations exist because there is no standardized testing protocol for examining bone mechanical properties. Without standardized protocols, most experimental protocols report essential procedures generically. For example, Kopperdahl [16] reports that "specimens were also cored parallel to the trabecular orientation." The process of determining the trabecular orientation was not mentioned. This omission presents an issue because research shows that misalignments of the trabecular orientation yield underestimations of mechanical properties [17]. A generic procedure like the above does not highlight the process of ensuring uniformity across fabricated test specimens. A solution to this issue is the use of more detailed protocols.

The premise of this work is, therefore, the experimental study of the effect of bone inorganic-organic composition on the mechanical properties. The results of this study will further enhance the knowledge of the mechanism of bone strength.

1.2   Aim of this Thesis

The main objective of this thesis is to experimentally investigate the effect of bone inorganic-organic composition on its mechanical properties. This work includes:

- Design of the testing fixtures and procedures.

- Sample preparation: managing anisotropy with a unique approach.

- Experimental test of cortical and trabecular specimens.

- Analysis of the inorganic and organic composition by a unique ashing procedure.

- Analysis of the effect of the inorganic-organic composition on mechanical properties.

1.3   Structure of this Thesis

This thesis comprises of 7 chapters.

Chapter 1 is the introduction, providing a brief overview of the motivation for the research topic, the objective of this work, and outlining the structure of this thesis.

Chapter 2 is the literature review, providing a comprehensive review of the existing relationships utilized in predicting bone strength and Young's modulus from bone density. Also included is a challenge currently faced in studying the effect of bone composition on mechanical properties. Next, in order to justify this work, the effect of organic content on bone mechanical properties is examined. Lastly, existing experimental protocols and their limitations are reviewed.

Chapter 3 provides an overview of the process for obtaining and storing bone samples, as well as details on the fabrication of cylindrical specimens.

Chapter 4 provides the details of the mechanical testing process and compositional analyses through bone Ashing techniques.

Chapter 5 provides the details of the statistical analyses conducted on fabricated specimens, ashed specimens, and mechanical tests.

Chapter 6 summarises the results from the analysis of the obtained data.

Chapter 7 is the last chapter of the thesis and provides conclusions, limitations, and suggestions for future work.

Chapter 2

Literature Review

Over the last few decades, bone research has shown significant signs of progress. These works have explored bone mechanical properties in meso, micro and macro scales due to the complexity of bone's behaviour and structure.

This chapter briefly reviews the topics which comprise of and support the basis of this thesis. Firstly, the existing relationships for quantifying bone strength from the density information are presented and examined. This examination reveals that the existing relationships might be missing a component necessary for accurate characterization of bone mechanical properties – organic content. Next, a major challenge (anisotropy) facing the study of the effect of bone composition on mechanical properties is addressed. This sub-section justifies why this research avoided the study of the contribution of anisotropy. Next, the effect of organic content on bone mechanical properties is explored. This sub-section justifies why organic content information might be the missing component in quantifying bone mechanical properties. Lastly, existing experimental protocols and their limitations are examined. The protocol review justifies the need to create a new protocol that includes organic content.

2.1   Density-Modulus Relationships

The most common tool for studying bone failure and assessing fracture risk is finite element analysis (FEA) [12,18–20]. However, the accuracy of FEA is profoundly affected by the material properties of bones under assessment [21–23]. An accurate characterization of bone mechanical properties – including the accuracy of local bone density information – is vital to making progress in the field [24]. As a result, the correlation of the mechanical properties of bone to their densitometric measures has been the focus of several studies.

The correlation between these mechanical properties and different densitometric measures is complicated. Mathematical models of these relationships have thus been developed from varying perspectives ranging from macroscopic (mm – cm) to microscopic (μm – mm) length-scales. Within these varying perspectives, relationships have been explored using tension or compression tests [25–32], bending tests [26,33,34], ultrasonic tests [31,35,36], and indentation tests [37,38]. This review will focus on the macroscopic length-scales perspective to expose a gap in these existing relationships. The microscopic length scales are currently beyond the scope of this work. At the macroscopic level, numerous studies have established strong relationships between bone Young's modulus and density. These relationships have been summarized by Helgason et al. [39]. The relationships he explored are not an exhaustive list of the existing relationships but a curated selection based on these inclusion criteria:

1. Human studies.

2. Explicitly stated mechanical tests performed on milled specimens.

3. Relationships established in text.

Most of the explored relationships follow a power-law relationship. The resulting mathematical model is a deterministic model simulating the relationship based on the analysis of small pieces of bone tissue [40]:

$$E = \alpha \rho_x^b, \quad \rho_x \text{ in } \left[\frac{\text{g}}{\text{cm}^3}\right], \quad E \text{ in [MPa]} \tag{1}$$

Where E represents the Young's Modulus and is utilized as the measure of elastic behaviour of bone samples, ρ_x represents the densitometric measure, with the subscript x standing for what kind of density information, α and b are generic constants determined by the researcher. The relationships utilize density information such as bone mineral density (BMD), apparent density (ρ_{app}), and ash density (ρ_{ash}). These densitometric measures are used because they have been established as positively correlated with Young's Modulus (E) [41,42]. The recurring densitometric measures used in the literature include apparent dry density, apparent wet density, bulk density, and ash density.

Apparent dry density or dry density, as used by Keller and Ciarelli et al. [27,43], involves defatting and drying the specimen. The dry weight is divided by the specimen volume. Apparent wet density or wet density or bulk density, as used by Linde et al., and Nicholson et al. [44,45], includes fluids that contribute to the overall mass but not its structural or load-bearing capability. In some cases, specimens are defatted of marrow and dried then rehydrated before weight measurement and testing. Both apparent dry and wet density definitions have commonly been referred to as apparent density, which adds another layer of complexity to the analysis of existing work. Ash density, as used by the existing body of research [27,43,45], involves incinerating the specimen and shows high reproducibility across protocols. Other relationships in the existing body of work [26,46–48] utilize bone

volume fraction (Bone Volume / Total Volume) instead of density. The alternative use of bone volume fraction is because it has been proven together with apparent density as a significant factor influencing bone strength and stiffness [49,50]. These different densitometric measures compound the difficulty of inter-study across the existing bodies of research.

Helgason et al. [39] investigated relationships by normalizing the above summarized densitometric measures to apparent density (ρ_{app}). An examination of the relationships reveals that the relationships differ vastly from each other even among similar animals and site locations. They discovered that methodological differences (including specimen geometry, testing protocol, and anatomical differences) alone could not explain the major discrepancies across studies. A possible explanation of the discrepancies might be that the developed mathematical relationships are missing a vital component. Existing biomechanical research of bone focuses on mineral content. This custom is because mineral content accounts for the structure of the bone, by composition. However, mineral content only accounts for 70% of the variation in the modulus [16,51]. Research has shown that the inclusion of other microstructural parameters might improve the estimation/prediction of E [29,30,52,53]. It was hypothesized that organic content is one such microstructural parameter. Organic content information could be the missing vital component of the developed mathematical relationships. To apply the mathematical relationships to whole bones, researchers investigate both cortical and cancellous bone. These bone densities range from 0.02 g/cm^3 – 2.00g/cm^3.

The power-law relationships (see equation (1) above) developed can be representative of the examined bone type. For cortical bones, the exponent b is typically higher than that

of cancellous bone which could be indicative of the tougher tissue structure of cortical bone. Nobakhti and Shefelbine [51] suggested that this could also be explained by representing cancellous bone with a cellular solid under bending loads; and a rule of mixture model for cortical bone. However, the rule of mixtures assumes that various phases in bone are composite and isotropic which is an inaccurate representation of bone. An accurate representation of bone would need to account for the anisotropic nature of bone. The following section addresses this challenge.

2.2   Study of Bone Composition Issue

An understanding of the contributing factors that influence mechanical properties is necessary for improving the empirical relationships. The difficulty in studying bone mechanical properties can be attributed to the complexity of bone [54]. This bone complexity can be classified as an internal factor. However, various factors (which can influence the intrinsic conditions of the bone) contribute to the difficulty, and can be summarised as: bone storage, preparation and handling [55]; testing set-ups [56–58]; orientation and anatomical location [17,59]; specimen geometry [44,60]; testing procedure [56,61,62]; and strain measurement [60,63,64]. The orientation issue arises because of the anisotropic nature of bone. Anisotropy is the property of bones that allows them to exhibit different mechanical properties when loaded in different directions/orientations. This behaviour would impede the collection of meaningful data if not appropriately managed. The study of the effect of

anisotropy was avoided in this research as it is beyond the scope of this work. To understand the magnitude of the contribution of anisotropy, an understanding of basic bone biology is necessary.

2.2.1 Bone Biology

Bones are composite materials that majorly exist to aid movement and provide mechanical support and protection to the body [65]. They also provide metabolic support like storage and mineral provision (like calcium). They consist mainly of an organic protein phase (type I collagen), inorganic mineral phase (carbonated hydroxyapatite), and water [66]. The inorganic mineral phase is responsible for the compressive strength of bone, while the organic protein phase is responsible for the tensile strength and ductility [67]. Structurally, collagen fibres, minerals and collagen are bonded together by non-collagenous proteins [68,69]. Anisotropic properties of bone can be attributed to the non-collagenous protein bonding, stress oriented collagen and the orientation of hydroxyapatite crystals in bones [70,71]. The nature of bone at different length scales provides an understanding of the anisotropic behaviour of bone.

Macroscopically, bone exists in two forms: cortical (compact) and trabecular (cancellous) bone. Cortical bones are typically found at the diaphysis and outer "shells" of bones, and trabecular bones are found at the metaphysis and epiphysis of long bones [67]. The macroscopic composition of bone (65% wt. mineral, 25% wt. organic, 10% wt. water [72,73]) is influenced by age, disease, anatomic site and diet. The anatomic site of bone

affects the anisotropy of bone since cancellous bones possess location-dependent anisot-ropy [74]. In contrast, cortical bones possess direction-dependent anisotropy. These aniso-tropic properties are a direct consequence of the microscopic composition of bone.

Microscopically, osteonal bone and periosteal bone can be found in bone and contribute greatly to the bulk mechanical properties of bone [71] (see Figure 1). Osteonal bone com-prises of osteons that align parallel to the long axis of bone [65]. Interstitial lamellae can be found in the space around osteons. Periosteal bone comprises circumferential lamellae that are parallel to the bone surface. Osteonal bone is known to be weaker and less aniso-tropic than periosteal bone [75]. The arrangement of these components of bone gives rise to bone's anisotropic properties. The anisotropic behaviour of bone is explored in more detail in the following section.
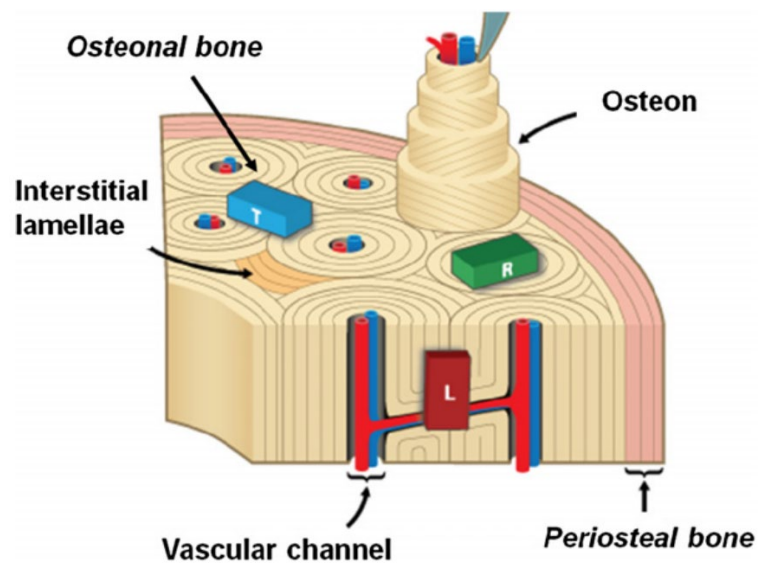
Figure 1: Bone sample orientations. L = Longitudinal. T = Transverse. R = Radial. Not to scale. [Novitskaya et al. 2011]

2.2.2   Anisotropic Behavior of Bone

Bone exhibits anisotropy due to its formation with its mechanical properties being different in its main directions: longitudinal (L), transverse (T) and radial (R) [76] (See Figure 1). As a result, research has been focused on investigating bone in the L, T and R directions [71].

Much work [30,46,77,78] has been done to prove that bone is anisotropic by loading bone at different orientations and measuring their mechanical properties (Figure 2). The
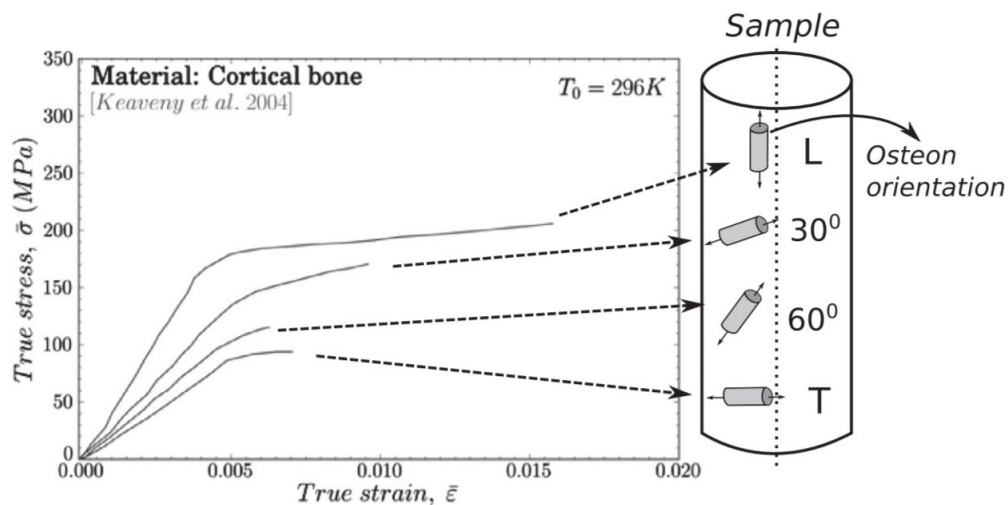
Figure 2: Anatomic orientation/osteon direction influence on the mechanical properties of bone. The hollow cylinder to the right represents a sample cylindrical specimen. Greyed smaller cylinders represent osteon orientation loaded in y-plane.[Santiuste 2014]

results show that the highest mechanical properties occur in the longitudinal direction in both cortical and trabecular bone. Reilly and Burstein [79] studied the anisotropic properties of cortical bone in compression and tension. They found that both the Young's modulus and ultimate strength in the longitudinal direction were nearly three times those in the transverse and radial directions. This finding is in agreement with Li et al. [80], whose work clearly shows that the longitudinal direction offers the best load-bearing capacity.

These results imply that mechanical testing in other directions would yield underestimations of the mechanical property. Several researchers thus investigated the contribution of misalignment of the longitudinal direction of the bone.

Ohman et al. [17] investigated the effect of main trabecular direction misalignment on Young's modulus and compressive strength of cancellous bones. They found out that a 20% misalignment was responsible for a 40% reduction in both Young's modulus and compressive strength. This effect of misalignment is in agreement with the works of Bonfield and Grynpas [78]. They studied the anisotropic behaviour of cortical bone at varying angles to the principal trabecular orientation (ranging from longitudinal as 0° to transverse as 90°) using ultrasonic techniques. They found that there was a gradual decrease in Young's modulus with increasing angles, with a plateau occurring between 20° and 70°. These findings justify the magnitude of the problem anisotropy brings to bone mechanism research. However, the contributions of the primary bone constituents need to be studied to understand the anisotropic behaviour of bone fully.

Hasegawa et al. [81] and Iyo et al. [82] investigated the contributions of these two main bone constituents to anisotropy. Hasegawa et al. [81] measured acoustic velocities on demineralized and deproteinized dog femur in both the longitudinal and transverse directions. They found that collagen exhibits little anisotropic behaviour, and mineral crystal contributes to most of the anisotropic behaviour. This finding, however, is in contrast with the finding of Iyo et al. [82]. Iyo et al. investigated the effect of anisotropy on the relaxation of Young's modulus of cortical bone in 3-point bending. They examined two processes: a slow relaxation process, attributed to a mixture of collagen and mineral phases, and a fast

one, attributed to the collagen matrix. Their results suggest that the former process (collagen and mineral phase mixture) was responsible for the anisotropic nature of bone [81]. Novitskaya et al. [83] confirmed the findings of Iyo et al. [82] with her work, which examined anisotropy of compressive mechanical properties of untreated, demineralized and deproteinized bovine cortical bones. They found that the bones all exhibit anisotropic mechanical behaviour. The longitudinal direction was the strongest for both demineralized and deproteinized bones. A possible explanation for the discrepancy in Hasegawa's findings lies in the isolation techniques used. The isolation techniques had not been well established in 1994 when Hasegawa's study was done, which means that the structural integrity of demineralized bone might have been compromised.

The magnitude of a single misstep due to the effect of anisotropy on mechanical properties has become more evident. This phenomenon is the case in Szabo and Thurner's work [84], where cortical bone tissue strains and microdamage were investigated in the three main anatomical directions using bending tests. They reported that the transverse direction yielded a higher Young's modulus than the radial direction – in agreement with existing literature. The transverse direction was defined as normal to bone growth, while the radial was defined as normal to both the longitudinal and transverse direction. However, they also reported that the Young's modulus in the longitudinal direction was equal to that in the transverse direction. This finding does not agree with the reviewed works in the previous paragraphs, and the larger body of literature. This discrepancy could be explained by the mechanics of bending deforming material. Since the bones deform in all directions through the induction of both compression and tension, their behavior in longitudinal and transverse directions appear similar. Another explanation for the discrepancy might be their technique

for aligning their samples to the longitudinal direction. It has been demonstrated that off-axis orientation can lead to decreases in Young's modulus and compressive strength [17]. Szabo and Thurner's method of fabricating samples might have led to some of their specimens being misaligned with the desired axis.

To obtain accurate results, researchers have sought to correctly ascertain and align their specimens with the principal trabecular orientation. The studies that examined empirical relationships between bone and its mechanical properties were also examined for the handling of anisotropy. Different techniques have been used so far, but they can be classified into two main classes: manual and digital. All the studies reviewed by Helgason et al [39] utilized various forms of visual inspection of their specimens to align them in the main trabecular orientation before cutting. However, Lotz et al. [85], determined trabecular orientation using CT scans. Digitized inspection techniques have been used by researchers to ensure higher alignment accuracy than manual techniques.

Bourgnon et al. [86] utilized a microscopy camera to ensure accurate alignment during their experiment. Morgan and Keaveny [59] quantified the degree of alignment using microCT scanning. Zhou et al. [87] ensured that the cylindrical axis was aligned to the trabecular orientation by utilizing x-ray radiographs on two orthogonal planes, parallel to the specimens. Majumdar et al. [88] also determined trabecular orientation using x-ray radiographs. The use of cameras and radiographs ensure misalignment is minimized. The drawbacks to utilizing these methods, however, are that they are both time-consuming and not necessarily readily available.

Visual inspections are cheaper but prone to human error. One such example is Schwiedrzik et al. [89], who reported yield stress values lower than literature values. This can be

explained by their utilization of bone specimens that were extracted perpendicular to the main trabecular orientation. Lv et al. [90] circumvented this issue by designing a custom mould for each femoral head used in their study to ensure extraction was from the same location for each bone. This process ensures higher precision and standardized sample extraction but is impractical for the preparation of large numbers of specimens [91].

The literature reviewed above shows that anisotropy is a major factor that can influence bone mechanical properties. However, the effect of anisotropy is beyond the scope of this work. Hence, the study of bone anisotropy was completely avoided by using a consistent process for fabrication of the bone specimens. This process would allow the focus of this work to remain on the study of bone inorganic-organic composition on its mechanical properties.

2.3   Effect of Organic Content

The organic content of bone was briefly introduced in sub-section 2.2.1 as the protein phase called type I collagen. Type I collagen protein is the flexible and ductile component of bone that is primarily responsible for tensile properties of bone [23]. Collagen is one of the constituents of the bone matrix. The bone matrix can be described simplistically as a two-phase system consisting of mineral hydroxyapatite held together by a collagen scaffold [54]. This viewpoint provides the understanding that in addition to providing the tensile strength, it is responsible for the mineral rigidity of bone since it serves as a template for the deposition orientation of the mineral component [92]. An examination of the individual properties of hydroxyapatite and type I collagen suggests that an optimal synergy is reached to attain the

superior macroscopic properties of bones [23]. The collagen fibres are stabilized within the bone structure because of their organization as parallel aligned, end-overlapped, and quarter-staggered molecules [93]. This organization structure is achieved by inter cross-linking and formation of minerals within the gaps of alignment. Thus, collagen inter-molecular cross-links have been thought to play a significant role in defining the mechanical properties of bone.

Many studies [92,94–97] in biomechanical research have examined reductions in bone strength and other parameters (like anisotropy) to determine variations not explained by bone density. However, only a minority of studies have investigated the biomechanical properties with organic content. Banse et al. [54] evaluated the mechanical properties of bone against the intermolecular cross-linking of collagen in adult human vertebral cancellous bone by compression. They confirmed that density information could not explain ~20-30% of the variation in modulus. They reported that differences in matrix composition could, however, explain a significant part of this variation. They further hypothesized that since non-collagenous proteins influence the quality and extent of mineralization, the mechanical properties of bone could be affected as well. They, however, failed to produce any valid correlations between compressive strength and organic content. This shortcoming was because they examined behaviour without accounting for the principal loading direction in their specimen fabrication. Other researchers examined the contribution of protein by investigating age-related changes.

Grynpas et al. [98] reported decreased protein production with age in their investigation of cancellous bones harvested from human femoral necks. They found that older individu-

als (aged 51 – 79 years) had less extracellular bone matrix proteins than younger individuals (aged 18 – 37). If the reduction of protein increases with age, organic content information could be one of the contributing factors to decreased bone strength with age. Mosekilde et al. [50] investigated age-related changes in cancellous bone quality that cannot be explained by bone density. They found that the biomechanical competence of the bone decreased significantly with age. They also investigated age-related changes in ash density differences. Their results show that changes in ash-density were not as pronounced as changes in biomechanical competence. These findings imply that organic content plays a significant role in the biomechanical property of bone. Mirzaali et al.'s work [38] with similar goals on cortical bone show that ageing did not affect microtissue properties. This result might be because they performed nanoindentation tests with a high order of magnitude for indentation – the former utilized compression tests. These findings elicited more profound attention in the field of bone research. Several works have, therefore, been executed at the nanoscale level to isolate either the mineral content or organic content before testing mechanical properties.

Chen and McKittrick [99] investigated the compressive mechanical properties of demineralized and deproteinized cancellous bone. They found that a strong synergistic effect was apparent from the interaction between the mineral phase and the protein phase. Novitskaya et al. [83] confirms this by proving that the weighted sum of demineralized and deproteinized bone is not equal to the strength of untreated bone. They further show that the Young's modulus decreased close to 100 times between the untreated and demineralized bones. This result affirms the contribution of the mineral component to bone stiffness.

However, the deproteinized bone did not have stiffness almost equal to that of untreated bone, and so, the contribution of organic content cannot be understated.

Since the contribution of organic content has been demonstrated to be impactful, work should be done to include it in biomechanical research. To effectively study the inorganic-organic composition on the mechanical properties of bone, a detailed process needs to be followed.

2.4 Existing Protocols and Limitations

The utilization of any experimental technique, whether compression or tension testing, requires strict protocols in order to produce useful and accurate data. As Helgason [39] identified, a large inter-study variation in experimental techniques for the completion of these tests exists. Examining the existing experimental protocols is therefore essential for identifying and resolving their limitations.

Section 2.2 briefly categorized the factors that influence the tested properties of bone. These factors – bone storage, preparation and handling, testing set-ups, orientation and anatomical location, specimen geometry, testing procedure, and strain measurement – are the reason inter-study approaches differ greatly. No standard for mechanical testing of bone has been established [15]. As a result, researchers [17,27,105–108,44,58,64,100–104] continuously modify existing protocols to achieve their research goals. While these researchers have documented their methods following strict journal article guidelines for methodology

summaries, reproducibility of experiments remains difficult. The protocols highlighted below consist of the various combinations of existing protocols and limitations associated with them.

Keller [27] described his approach for uniaxial compression of cubical specimens of human vertebral bone and femoral bone (n = 550). Samples are stored at –30°C after machining. Temperature and moisture are controlled with a continuous 0.9% saline irrigation. The bones are tested as close to physiologic conditions as possible in order to obtain results close to in-vivo performance. However, Keller failed to document the process for maintaining physiologic conditions in this work of literature. Specimen dimensions (width and height) are collected using a digital calliper (± 0.003mm). The specimens are visually inspected before mechanical testing in uniaxial compression. Oil is used on the platens before loading the specimens. Loads are then applied to the specimens, which are aligned with their primary loading axis. However, the process for determining the primary loading axis was not documented. The specimens are then tested until a reduction in load is observed. Keller, however, did not precondition the samples before testing. Current work [64] shows that not preconditioning specimens results in gross underestimation of compressive Young's modulus. Following mechanical tests, both dry and ash densities are obtained after the use of a muffle furnace at 100°C (1 hour) and 650°C (18 hours), respectively.

A variation of the above procedure was used by Linde et al. [44,61,102] during his experiments. He studied the effect of storage methods and specimen geometry on the mechanical behaviour of bones and utilized both cylindrical and cubical specimens (n > 74). The samples are stored at –20°C and thawing time of 2 hours is used before testing. A conditioning procedure is followed to 0.4% strain to obtain optimum mechanical property

results. Linde's experiments also differed slightly than Keller's in terms of the post-mechanical testing phase – the use of an air jet for blowing the bones free from marrow as opposed to a water jet. Ouyang et al. [105] followed a similar procedure with a minimum thawing time of 2 hours, while specimens remained in ringer's solution. However, both Linde and Ouyang completely omitted the drying and ashing processes from their procedures. This conclusion was reached after examining both the outlined methodology and the results of the experiments.

Ohman et al. [17] examined the off-axis measurement effect on the mechanical properties of cylindrical bone specimens. They extracted cylindrical bone specimens from the head of femur bones using a newly developed protocol. The extraction method ensured less than 10° misalignment error along the main trabecular direction of the bone. However, the process is only well suited to femoral heads and cannot be easily re-purposed for other parts of bone, especially long shaft bones. Storage procedures were not mentioned in this body of work. It is possible the prepared specimens were not frozen before testing because the protocol reports that the bones to be tested are left in ringer's solution for an hour before testing. This might have been done to maintain the tissue hydration of the bone. The mechanical tests followed already established end-cap techniques to minimize errors due to end effects. Ashing is performed at 650°C for 24 hours after preliminary testing to determine the optimum temperature at which ash weight made no significant change.

A shortcoming of the protocols mentioned above is the limited documentation of specific vital steps. Inter-study reproducibility is more complicated, taking into account the various complexities that arise with the different combinations of approaches that could be

taken. For context, during compression testing alone, about 6 different compression methods – platen compression, undersized platen compression, sleeve-constrained compression, epoxy-platen compression, epoxy-embedded compression, brass-endcap compression [109] – have been identified across literature with each possessing unique shortcomings Furthermore, the limitations outlined in this chapter surrounding bone mechanical testing research compound the complexity of experiments. Detailed protocols need to be outlined in order to provide an avenue for increased success in testing and repeatability across research groups.

2.5   Objective of this Work

Numerous approaches for studying the mechanical behaviour of bone have been devised and well-established. These approaches do well to describe the mechanical properties of both trabecular and cortical bones. However, there may be a missing link fundamental to the mechanical behaviour of bone – organic content information. Empirical relationships that incorporate the organic content information do not exist in literature to the best of the author's knowledge. To fill this gap, careful consideration must also be taken to minimize the contribution of anisotropy to produce meaningful data. Furthermore, the challenges analyzed in this review make future experiments difficult. This work seeks to therefore establish strict processes, to be used to facilitate the investigation of the effect of organic content in tandem with inorganic content. Steps to ensure consistency in dealing with anisotropy were taken and can be seen in section 3.2.

The following chapters (3 – 5) present the methods utilized in this study from the collection phase to the testing and analyses phases.

Chapter 3

Bone Sample Preparation

The specimen fabrication method is crucial to maintaining the integrity of the mechanical property of the bone samples under assessment. Such care is needed because these mechanical properties depend on mineral and organic content, and can be altered by anisotropy, moisture, and temperature [23,110].

This chapter presents the methodology for the completion of this work. The chapter is structured to show how the effect of anisotropy is minimized by the fabrication procedure. Beyond the reduction of the effect of anisotropy, the chapter also shows how the effects of moisture and temperature were minimized.

The chapter outlines the methodology for the acquisition of bone samples and the fabrication of the bone specimens from these samples. A summary of the procedure is presented in Figure 3. The methodology for mechanical testing and analysis are presented in subsequent chapters.

Start

| Acquire Bones | → | **Fabrication of cylindrical test specimens** |

Store. At -20°C until fabrication

Embed. Follow steps to embed whole bone in mould.

Machine Sections. Cut the embedded bone into section lengths equal to the length of the trephine.

Is section ~ length of trephine?   → No →   **Discard**

Yes

Core Cylinders. Core the cylindrical specimens from the rectangular blocks using the trephine attached to a drilling machine.

Discard   ← Yes ←   Are there physical damages? Are surfaces unsmooth and/or unparallel?

No

Label. Label the fabricated specimens according to a pre-set naming convention for uniformity.

Wrap in Cling Film.

Store. Store in airtight container at -20°C until needed for mechanical testing.

Finish

Figure 3: Procedure for the fabrication of bone specimens utilized in this study.

3.1   Acquisition and Storage of Bone

Bovine limb bones (herein referred to as "bones" for simplicity) were sourced from a local abattoir – St. Claude Abattoir, in Manitoba, Canada. The abattoir's butcher removed tendons and surrounding soft tissue of the bones. This soft tissue removal was conducted without scraping off the bone itself as that would affect the properties of the bones being tested – effectively weakening them. The bones were frozen and well-documented by the butchers using a prepared document (see Table 1 below). The gender of some of the cows were not recorded by the butchers at the time of death. Thirty-six bones were sourced in total and utilized in this study. Following the literature guidelines [110–112], the collected bones were stored at -20°C. Linde and Sorensen [55] found that storage at this temperature yielded no significant effect on the mechanical properties of bone.

Table 1: Information of Cows.

Animal [ID]	Breed	Age at slaughter (months)	Gender	Weight (lb)
1	Black Angus	16-18	Female	950-1050
2	Black Angus	16-18	-	950-1050
3	Black Angus	16-18	-	950-1050
4	Jersey	14	Male	800-900
5	Simmental	16	-	1205
6	Black Angus	16-18	Male	1000
7	Jersey	14-16	-	800-900
8	Red Angus	12-14	Male	800
9	Simmental	18	-	1597

3.2   Fabrication of Bone Specimens

Bone samples were harvested from the fresh cadavers obtained from the butchers. The samples were inspected before fabrication. They showed no visible conditions that would adversely affect their properties. Residual soft tissue was removed from the samples before the fabrication process. The cadaver anthropometric data is reported in Table 1. According to the Public Health Agency of Canada (PHAC) [113], handling of biological tissue requires attention to health and safety to avoid the risk of diseases and infections spreading. The collection and handling of the bone samples were conducted according to PHAC and the recommendations of the World Medical Association, as concluded in the 52nd General Assembly of the World Medical Association. Personal protective equipment was used to protect against the generation of bone chips, and aerosols.

The bovine samples were not allowed to thaw due to the nature of this procedure. The use of frozen samples is of vital importance to the preservation of moisture in the fabricated specimens. Existing research involves hydrating the bones with physiological saline after a drying procedure has occurred. The approach followed in this research completely removes the need to re-hydrate by maintaining the moisture content of bone. The frozen samples were only thawed to room temperature when they had been fabricated and ready for testing. Cylindrical bone specimens were cored out of the frozen bone samples. The bone cores were obtained at an optimum speed such that minimal heat was generated. This step was critical to reduce any moisture loss from heat generation. With a procedure for managing moisture in place, the fabrication of the bones was completed keeping in mind the anisotropic nature of bone.

A procedure for obtaining consistent cylindrical specimens from the bone samples while avoiding the effects of anisotropy was devised and is explained below. Keeping the orientation of the bone constant for all bone femur samples obtained is crucial to obtaining a uniform manufacturing process and minimizing the effects of anisotropy. A reference system was used in order to achieve constant orientation across the collected bone samples. The proximal femur anatomy was utilized as the basis for creating a reference system in order to obtain consistent alignment of the samples. This step is crucial because, as shown in Section 2.2.2, human bones are highly variable internally from site to site, and properties change depending on loading direction.

The setup used to manage anisotropy and obtain consistent alignment can be seen in Figure 4 and Figure 5. First, a sizeable transparent tarp (4-1/2 Feet × 75 Feet Clear 8 mil Ultra Multipurpose Vinyl, Home Depot, Winnipeg, Canada) was set on the lab workstation table to protect the surface. A rectangular mould comprising of 4 pieces of unfixed wood roughly 16cm (tall), 60cm (long) and 17cm (wide) – enough to house an entire bone – was

Figure 4: Mould Frame + Bone Setup
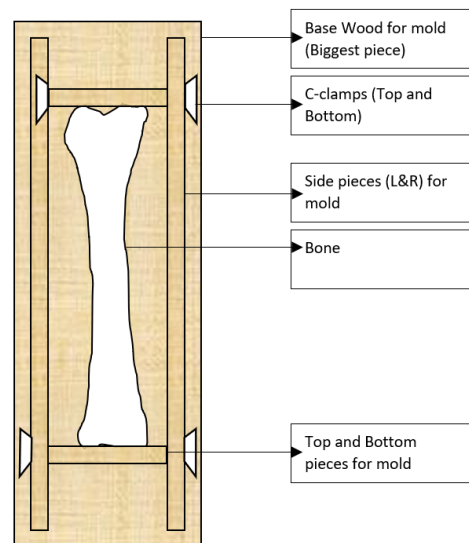
Figure 5: Schematic of the mold setup

then set down on the prepared table (thickness = 1cm). The bone was then placed on the table surface on its anterior side noting that the protruding head of the femur faced upward. This step is crucial to ensuring the orientation remains the same through every prepared specimen. The corners of the mould, where the ends of the smaller mould components met with the longer mould components, were then tightly sealed by using C-clamps, as illustrated in Figure 4. An additional piece of wood was then used as a base for the mould frame and placed on the table. The entire clamped frame together with the bone inside the enclosure was then placed on the base to secure the bottom (Figure 5). In this orientation, the longitudinal shaft axis is, therefore, always parallel to horizontal plane.

With the bone in the enclosure, the bone was embedded in a Plaster of Paris mixture. Plaster of Paris was used because, in addition to being cheap and readily available, it is a biocompatible material that can be considered a bone mineral [114]. The mixture was allowed to set in the mould for 45 – 60 minutes before the clamps and surrounding wooden components were removed. The purpose of creating rectangular moulds was for ease of manipulation and consistency during the fabrication process. The rectangular femur mould (see Figure 6) was cut into sections of approximately 32.50mm using a 30cm miter saw (laser, Ryobi, Inc.). The section length was determined by the length of the drill bit to be used to core out the cylindrical specimens.

The proposed specimen geometry was cylindrical, as existing research has shown that they yield highly repeatable results [44]. The specimen dimensions were taken based on ASTM standards. The specimens were cored out of viable parts of the rectangular sections using a 25cm drill press (laser, Ryobi, Inc.) with a cylindrical trephine (32mm × 8mm) as

the drill bit. The drill press was rigged such that the cut section could be clamped in place using 5cm × 10cm clamps (Stanley, Inc.).
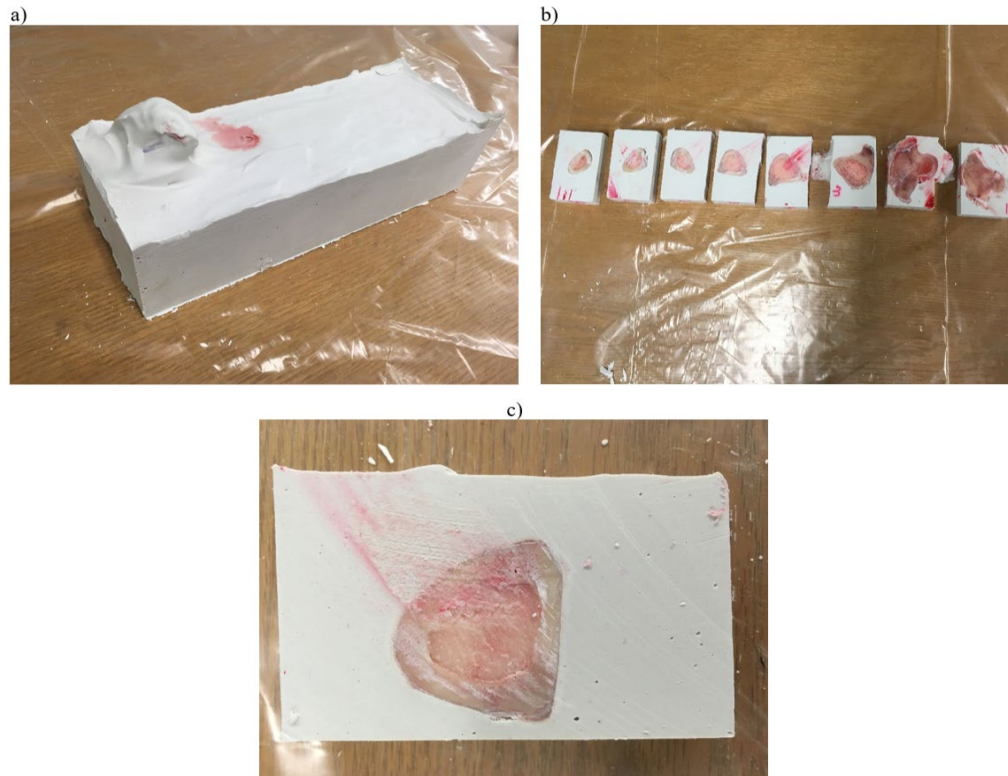
Figure 6: a) Dried mould with the entire bone embedded. b) The cut mould sections. c) Close-up of one of the cut sections which is characterized by smooth surface cuts.

The cylindrical specimens were cored out while the sample was still frozen since a clear boundary of bone and marrow content could be easily seen, allowing for ease of fabrication. Since the bone was embedded in a single orientation, the long axis of the cored specimens is always parallel to the longitudinal axis of the whole bone, thus eliminating the concern of the anisotropic behaviour of bone. The cored-out specimens were then labelled by animal number and specimen number in the format "A#N#"; where A# represented the number we had given the animal the bones were obtained from, and N# represented the corresponding number of that viable specimen. They were then wrapped in

cling-film to keep moisture in and placed in airtight containers that were labelled for just the animal numbers. This way, the specimens were stored in different enclosures while ensuring specimens did not get mixed up between animals. 107 cortical and 182 cancellous bone specimens were obtained. The specimens remained in -20°C and were thawed to room temperature when needed for testing. This was to ensure that temperature variation was consistent among specimens.

Chapter 4

Mechanical Testing and Ashing

This chapter reports the methodology for carrying out mechanical testing and ashing on the fabricated specimens. Bones exhibit different intrinsic properties in compression and tension; therefore, the fabricated samples were sorted by density, and then split equally into two groups. Compressive tests were performed on one group, and tensile tests were performed on the other group. Both tests involved the application of a uniaxial force on the specimen with the force and strain measurements recorded for the determination of the intrinsic material properties [115]. These tests were chosen for consistency with the existing research and ease of comparison. However, 2 key assumptions regarding the fabricated specimens to be tested were made:

1. The density across each individual specimen is uniform.

2. The corresponding stress distribution across the specimen will be uniform.

This assumption can be summarized as bone being treated as a homogenous material. However, bone is not a uniform material. The analysis of bone as a non-uniform material would require more complex techniques that is beyond the scope of this work. Therefore, the results must be interpreted with this assumption taken into consideration.

4.1   Compression and Tension Tests

The fabrication process presented in the previous chapter was explicitly designed to target and minimize issues arising from anisotropy. Since bone tissue is not uniform across the bones, the fabricated specimens had different densities. Some preliminary validation tests were performed on specimens excluded from the experiment. These tests served multiple purposes: to determine the effect of defrost duration on the density; to determine testing parameters – strain rate, pre-loading force, Young's modulus calculation equation; to calibrate the machine being used (following ASTM calibration standards for compression and tension [116]), and to test the accuracy of the mechanical properties obtained. It was determined that the specimens would be left out to defrost at room temperature for 10 hours before testing.

The thawed specimens were tested in groups of 14 since this is the capacity of the muffle furnace to be used for ashing. Physical measurements were taken using callipers ($\pm$ 0.001) and recorded in a prepared test form (Appendix A). An electromechanical material testing system (MTS Insight 30, MTS Systems Corporation, Eden Prairie, MN, USA) equipped with a 30kN load cell was used for compression tests (Figure 7).
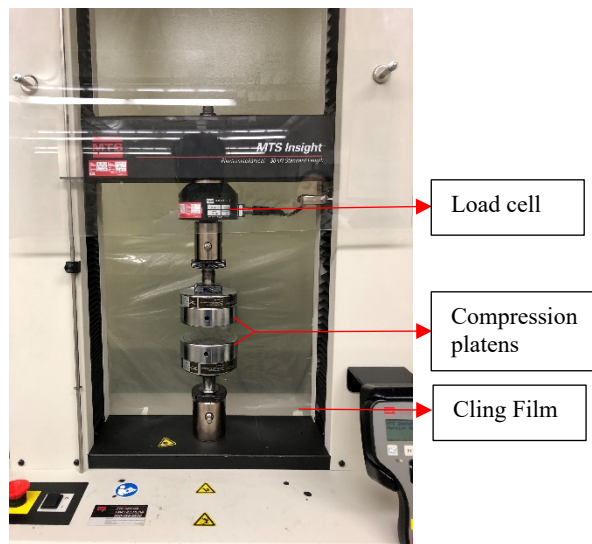
Figure 7: MTS material testing system.
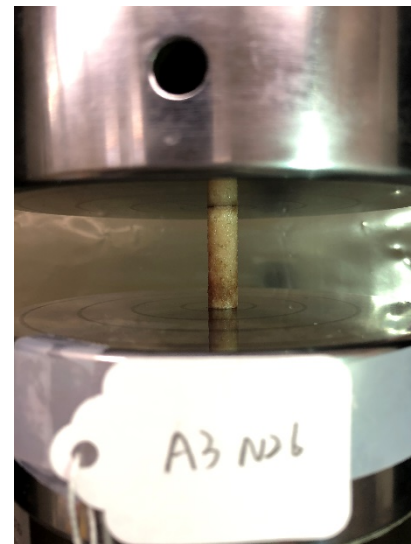
Figure 8: Compression test setup with a sample cylindrical bone specimen. Labels are used to ensure sample data are not misattributed.

The setup included a set of compression platens: a fixed lower platen and an upper adjustable one. Specimens were tested by uniaxial compression (Figure 8) to failure or 3mm compression displacement at a crosshead speed of 1.50mm/min (equivalent strain rate = 0.0033/s) in unconfined conditions. The strain was automatically calculated by the accompanying software (TestWorks 4^{TM}, MTS Systems Corporation, MN, USA) from the displacement of the compression platens.

A customized testing profile was created to comply with ASTM Standards [117–121]. The machine was calibrated before tests. In testing, the specimen was preloaded with 50N force to ensure that they were in full contact with the platens. The specimen being tested was placed on the fixed lower platen. The upper adjustable platen was then used to apply a load of less than 50N to the specimen in order to induce strain levels less than 0.5% [91]. The tested mechanical properties included: Young's modulus, yield stress, break stress,

ultimate stress, and energy to yield. The file was saved with a naming convention consistent with the label of the tested specimen – A#N#.

The tension tests were conducted in a similar manner as the compression tests. The main differences from the compression tests are outlined below. The MTS machine was mounted with tension grips (MTS Advantage^{TM} wedge set, 7 to 12.7mm diameter, serrated profile, MTS Systems Corporation, MN, USA) for a greater contact surface area (Figure 9).
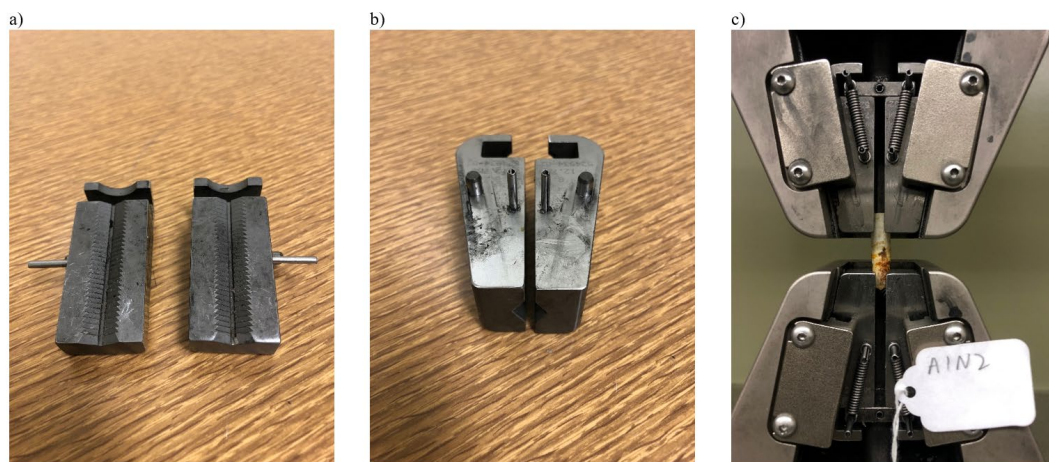
Figure 9: a) and b) show the face and side profiles of the custom tension grip utilized in grasping the fabricated cylindrical specimens. c) shows a cortical specimen held by the grips for tension testing.

Specimens were tested by uniaxial tension loading to failure or 3mm extension at a cross-head speed of 1.50mm/min in unconfined conditions. The bottom of the specimen was first loosely gripped to keep the specimen erect. It was essential to not induce unnecessary stresses into the specimen, which could adversely affect the mechanical behaviour. The top grip was then lowered and tightened. Next, the bottom grip was tightened to ensure the specimen was secure before running the test. The average gage length (14mm) used was estimated using the shortest specimen (27mm) with the grips specified in Figure 9 above. The grip ends at the top and bottom accounted for approximately no more than 13mm of

bone surface area to be gripped. This is because smaller surface areas allowed for slippage, especially on the cancellous bone specimens.

4.2   Composition Analysis – Bone Ashing

Prior to mechanical testing, the muffle furnace (thermolyne 47900 Eurotherm, Thermo Fisher Scientific, NC) volume was determined as 5.735×10^6 mm^3. The volume was obtained to determine how many crucibles could fit (n = 14) at a time. This decided the number of specimens to be evaluated per testing period (n = 14). The furnace was prepared for the ashing stage by thoroughly investigating its working conditions. This analysis can be found in Appendix B.

The end of mechanical testing for a set of specimens signified the start of the last stage of testing: composition analysis by bone ashing. At high enough temperatures, the organic content of bone can be burnt out, leaving just the inorganic mineral content. Therefore, ashing was done to obtain the inorganic and organic content information of the bones. The tested bone specimens were handled according to protocol specifically designed to analyze the content of the bone through ashing techniques. The steps were created after reviewing relevant literature [23,122]. The specimens were placed in ceramic crucibles that had been numbered to correspond with their label system (Figure 10). They were then placed in the muffle furnace at 700°C for 20 hours. Those parameters for the ashing procedure were

determined after testing combinations of temperature (600°C – 750°C) and duration (16 –

24 hours) seen in literature.
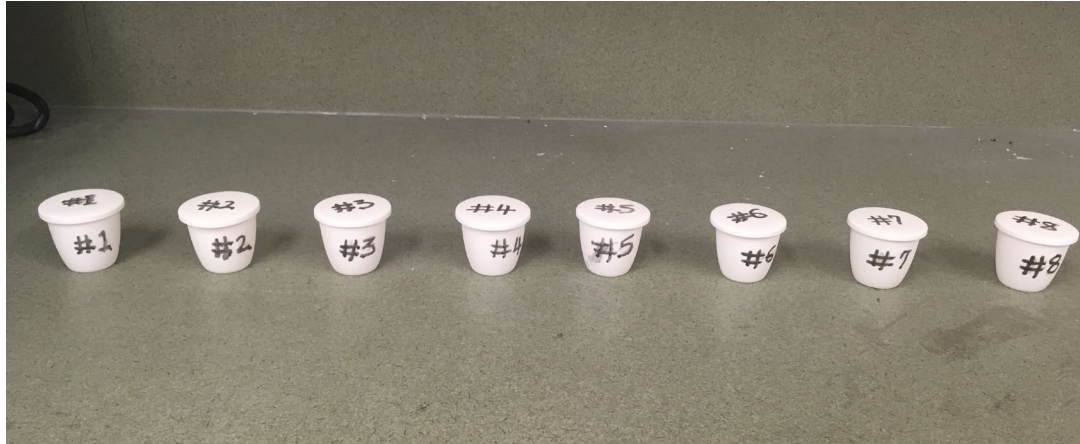
Figure 10: Image of crucibles + covers. Both the crucibles and their corresponding covers are numbered to protect the integrity of each specimen.

Chapter 5

Statistical Analyses

This chapter outlines all the analyses undertaken for the various stages of testing in this work.

5.1 Fabrication

The physical properties of the fabricated specimens (length, diameter and weight) were obtained using digital Vernier callipers and weight scales as average of 2 measurements (Table 2). This method of physical measurement was to account for any inhomogeneity of the specimens. The precision of the fabricated specimens was evaluated using the standard error of the mean of the physical measurements.

Inter-specimen type (cortical vs cancellous) length and diameter differences were investigated using 2-samples t-tests. The t-tests were conducted since research has shown varying effects of specimen length and diameter on the Young's modulus of bone [44,109].

The apparent wet density of the specimens was calculated from the physical property measurements using:

$$apparent\ density = \frac{mass}{wet\ bulk\ volume} = \frac{m}{\Pi \times r^2 \times l}$$

where mass (m) was the weight of the specimen in grams, and the volume was defined by radius (r) and length (l) of the cylindrical specimen in mm.

Density information has been strongly linked to the Young's modulus of bone [41]. A separate t-test was conducted on the compression and tension group specimens to account for any variations between testing groups.

Table 2: Summary of the mean physical measurement dimensions of the specimens used in both compression and tension. The bones were sorted by bone types into cortical and cancellous since the behaviour of bones is affected by their type.

Bone Type	Attributes	Cortical	Cancellous
Compression	No of specimens	59	92
	Length (mm)	28.07 ± 3.52	27.73 ± 3.59
	Diameter (mm)	7.84 ± 0.20	7.88 ± 0.57
Tension	No of specimens	48	90
	Length (mm)	28.89 ± 2.06	28.59 ± 1.97
	Diameter (mm)	7.74 ± 0.24	7.76 ± 0.34

5.2   Bone Ashing

The densities and content information were calculated using the following descriptions:

- Ash density = ash weight/ total volume

- Contents:

    Ash content = ash weight

    Organic content = hydrated weight – ash weight

A one-tailed paired t-test was performed on the before-test and after-test hydrated weights to confirm see if they were different from each other. This was important because sample loss is always expected in a destructive testing method.

5.3   Mechanical Testing

SPSS (IBM SPSS Statistics, Version 24.0, IBM Corp., Armonk, New York) was used for all analyses taking $p < \alpha = 0.05$ as significant. Prior to testing, the samples were split randomly into compression and tension. Independent samples t-tests were conducted on the lengths, diameters, and densities to confirm that there were no differences between them.

The Young's modulus was calculated as the slope of the linear portion of the stress-strain curve generated by TestWorks^{TM}. Stress was calculated as the load divided by the area of the cylindrical specimen. Since the current body of work utilizes regression analyses to explore the relationship between bone density and its mechanical property, regression analyses were conducted in compression and tension and grouped by bone type: cortical, cancellous, and pooled (cortical and cancellous). The Young's modulus and peak stress were plotted as functions of ash density and both linear and power-law regression analyses were conducted. The Young's modulus and peak stress were plotted as functions of organic content density. The Young's modulus and peak stress were then plotted as a function of density ratio (ash/organic density). The corresponding regression analyses were also conducted. The coefficient of correlation (R) and coefficient of determination adjusted for degrees of freedom (adjusted R^2) were calculated for each regression. The level of correlations for mineral content (ash density) and density ratio (ash/organic) were directly

evaluated against each other. This was to evaluate the efficacy of the parameter in determining mechanical properties.

The analyses highlighted above serve to achieve the objective of this thesis by doing four things: First, it collects similar data as the existing body of work by the regression analyses of the ash density-modulus and ash density-peak stress relationships; Next, it collects data that explores the direct relationship between organic density and mechanical properties (modulus and peak stress). This data is also obtained through the regression analyses between the variables. Next, it explores the relationship between the interaction of ash density and organic density (ash density/organic density) and the mechanical properties through a regression analysis. Lastly, the results are compared with each other but also evaluated independently. The results obtained from the analysis would, therefore, serve to enhance the body of knowledge which has been lacking the contribution of organic content.

Chapter 6

Results and Discussion

The previous chapters illustrate the methodologies utilized in the fabrication and testing of bovine specimens. In this chapter, the experimental results arising from the application of those methods are presented and examined in detail.

The results are presented in different groups for compression and tension where applicable. The Fabrication technique is evaluated by examining the fabricated specimen differences and is presented in Section 6.1 below. Due to the application of destructive compression and tension tests, evaluation of sample loss is presented in Section 6.2. Results from the study of the mechanical behaviour of tested specimens in compression and tension are then presented by isolating inorganic, organic, and inorganic-organic interactions with the mechanical properties in Section 6.3.

An upper threshold of significance value of $\alpha = 0.05$ is used for all statistical analyses.

6.1   Fabricated Specimens Differences

A large specimen-set and modifications of existing protocols were utilized in this study. To provide validity to these protocols (beyond the fabrication method described in Subsection 3.2), it is essential that some statistical test is conducted to assess uniformity across specimens. The uniformity of the specimens is important because research [44,109] has shown that bones behave differently depending on density, length and diameter. Three main parameters therefore need examination before further analysis can be conducted: density, length and diameter.

Existing research [33,97,123–125] utilizes grouped cross-sections in obtaining specimens, thereby allowing uniformity of density information. The common cross-sections are the proximal femur, distal femur and proximal tibia. Other cross-sections are further subdivided into four anatomic quadrants: anterior, medial, posterior, and lateral [80]. However, in this study, specimens were obtained across the spectrum of each whole bovine bone sample and not grouped by cross-section. Although the specimens were grouped with similar density into tension and compression, it is vital to assess any differences in density between both groups in order to ensure an even distribution of specimens to both groups.

Furthermore, studies have shown that specimen length and diameter have significant influences on the mechanical behaviour of bone [44,109]. Lievers, Waldman, and Pilkey [109] investigated the minimization of specimen length in the elastic testing of end-constrained cancellous bone and found that diameter strongly affected the apparent modulus ($p = 0.0005$). A decreasing specimen length was found to accompany decreasing Young's modulus during platen compression [44]. Differences in sample length and diameter could,

therefore, skew the mechanical behaviour, so assessing and categorizing results accordingly would be valuable.

6.1.1   Differences between Length and Diameter

Since research [44] has shown that an underestimation of Young's modulus is obtained with decreasing specimen length, in order to obtain accurate estimations of Young's modulus, it is essential that differences in length are not significant between the cortical and cancellous cohorts being studied in either compression or tension. The differences in length were assessed using the cortical and cancellous cohorts because the distribution of lengths at those levels, were random. The hypothesis test to determine any significant difference between these groups is the 2-sample t-test, which directly tests the average difference between the two groups.

A 2-sample t-test was thus conducted on the compression group to determine whether the fabricated cortical specimens were different from the fabricated cancellous specimens (using length and diameter as fabrication determinants). The summary of the test is presented in Table 3. The results indicate that the mean length of the cortical group ($M = 28.07$, $SD = 3.52$) was not significantly different than that of the cancellous group ($M = 27.73$, $SD = 3.59$), $p = 0.575$, 95% CI [-0.84, 1.51]

Similarly, the mean diameter of the cortical group ($M = 7.84$, $SD = 0.20$) exhibited non-significant differences from the cancellous group ($M = 7.88$, $SD = 0.57$), $p = 0.533$, 95% CI [-0.17, 0.09]. These conclusions allowed confidence in the fabricated specimens. Specimen length and diameter were, therefore, not used as confounding variables in the study since they were not significantly different within their cohorts.

Table 3: Summary of the independent samples' compression t-test for equality of means between cortical and cancellous bones utilized. This test was done for both length and diameter.

Attributes	Mean diff (mm)	SE	95% CI		*p*-val. (2-tailed)
			Lower	Upper	
Length	0.3341	0.5915	-0.8365	1.5048	0.573
Diameter	-0.0406	0.0649	-0.1691	0.0879	0.533

The tests were not conducted for the tension group since the fabrication process was the same.

6.1.2   Difference between Densities

The samples were grouped by density for compression and tension testing. To further validate the fabrication process and ensure consistency across tested samples in the testing groups, t-tests were performed. Beyond validating the fabrication process, the relationship between apparent density and Young's modulus has been established – Young's modulus of bone is strongly dependent on apparent density [25]. Although compressive and tensile tests have been shown to yield different results, there is little work to show the equivalency of specimens tested in both compression and tension. The t-test was conducted to account for any possible differences between compression and tension groups.

An analysis of the compression and tension apparent densities shows that the groups did not differ significantly, $p = 0.189$, 95% CI [-0.02. 0.12]. The summaries of the apparent density measurements and statistical analysis are presented in Table 4 and Table 5 below.

Table 4: Summary of the analyzed density information for compression and tension specimens. N stands for sample size.

Attributes	N	Mean (g/cm³)	Std. Deviation	Std. Error Mean
Compression	189	1.663	0.4049	0.0294
Tension	178	1.614	0.3123	0.0234

Table 5: Summary of the independent sample of density t-test for equality of means*.

Attributes	Mean diff (mm)	SE	95% CI		p-val. (2-tailed)
			Lower	Upper	
Density	0.0495	0.0376	0.0245	0.1235	0.189

*Abbreviations: SE stands for Standard Error of the mean difference.

   CI stands for confidence interval.

   p-val stands for the significance level. An $\alpha = 0.05$ was utilized to accept significance.

6.2   Mechanical Testing Results

Following mechanical testing, an ashing procedure was conducted to obtain the ash weight (and conversely, density) of the tested specimens. To accurately assess the relationship(s) between the ash density (and future results post-mechanical testing) and modulus, it is crucial that the integrity of the specimen (mass-wise) is maintained. Significant sample loss would skew the mechanical behaviour analysis significantly. In order to both verify and combat errors due to sample loss, an analysis of possible loss needed to be conducted.

   A one-tailed paired samples t-test was therefore conducted to determine whether the weight of the samples measured before and after mechanical testing were significantly different from each other. It was hypothesized that sample loss (including moisture loss) during the destructive testing process would render weight measurements significantly different (more specifically, the weight after test would be less than that before test). After testing

the homogeneity of variances using pitman-morgan's test ($R^2 = 0.99$, p = 1.953), the specimens had an average difference from pre-test to post-test measured weights of 0.0665 (*SD* = 0.0717), resulting in a statistically significant weight difference ($p < 0.0001$). The sample loss however, was considered negligible (3%).

Table 6 and Table 7 show the summaries of this analysis.

Table 6: Summary of the analyzed weight data (pre- and post-mechanical tests). N stands for the sample size.

Attributes	Mean (g)	N	Std. Deviation	Std. Error Mean
Weight$_{Pre-Test}$	2.226	367	0.5058	0.0264
Weight$_{Post-Test}$	2.160	367	0.5133	0.0268

Table 7: Summary of the paired samples t-test analyzing the difference between pre- and post-mechanical test weights*.

Attributes	Mean (g)	SD	SE	95% CI		*p*-value
				Lower	Upper	
W$_{Pre}$ - W$_{Post}$	0.0665	0.0717	0.00374	0.0591	0.0738	0.000000

*Abbreviations: SD stands for Standard Deviation, SE stands for Standard Error of the mean difference
CI stands for confidence interval.
p-val stands for the significance level. An $\alpha = 0.05$ was utilized to accept significance.

6.3   Mechanical Properties

6.3.1   Compression

The properties (Young's modulus, yield stress, break stress, ultimate stress, ultimate strain, and energy to yield) obtained from compression tests are summarized in Table 8 and Table 9 below, including ash density information.

Table 8: Summary of the obtained elastic properties of cancellous bones in compression.

Cancellous		E (MPa)	ρ (g/cm³)	σ^peak(MPa)	σ^Break (Mpa)	σ^yield(MPa)	Y^Energy (N.mm)	ρ_ash (g/cm³)
N	Valid	89	92	89	59	89	89	92
	Missing	3	0	3	33	3	3	0
Mean		1450.014	1.411	12.357	13.138	12.067	225.589	0.490
SE		68.208	0.025	0.915	1.262	0.916	27.049	0.015
Minimum		126.761	1.072	0.300	0.342	0.334	0.352	0.193
Maximum		3127.644	2.300	50.800	50.788	50.788	1646.265	0.846

Missing: the number of specimens that did not produce any output.

Abbreviations: N = sample size, SE = Standard Error of the mean.

   Y^{Energy} = Energy to yield.

Table 9: Summary of the obtained elastic properties of cortical bones in compression.

Cortical		E (MPa)	ρ (g/cm³)	σ^peak(MPa)	σ^Break(MPa)	σ^yield(MPa)	Y^Energy (N.mm)	ρ_ash (g/cm³)
N	Valid	59	59	59	52	59	59	59
	Missing	0	0	0	7	0	0	0
Mean		7191.689	2.073	128.353	138.110	122.887	1880.507	1.234
SE		314.056	0.041	6.163	5.634	6.716	120.826	0.026
Minimum		1284.985	1.438	21.100	30.223	7.717	21.773	0.668
Maximum		11658.365	3.349	198.100	198.149	198.149	4330.616	1.934

Missing: the number of specimens that did not produce any output.

Abbreviations: N = sample size, SE = Standard Error of the mean

   Y^{Energy} = Energy to yield.

The average Young's modulus of cortical bone in compression is almost five times that of cancellous bone in this work. The average ultimate and break strength of cortical bone are about ten times that of cancellous bone. The range for ash density, including both cancellous and cortical bone, is 0.193g/cm³ to 1.934g/cm³.

An outlier analysis was performed on the relationships between ash density and Young's modulus for pooled (cortical and cancellous), cortical and cancellous bones. The results were not statistically different from the results obtained from the inclusion of the outliers. The regression curves for all relationships with the exclusion of the outliers are thus presented.

The power law model used for curve fitting was $y = \text{Constant} \times x^{b1}$ where y is the dependent variable (either modulus or peak stress), x is the independent variable (density), and b_1 is the exponent. The results from this power-law relationship indicate that the ash density and Young's modulus are strongly positively correlated ($R = 0.89$, $R^2 = 0.78$) for pooled bones. Cortical bones ($R = 0.72$, $R^2 = 0.51$) and Cancellous bones ($R = 0.43$, $R^2 = 0.18$) show medium and low positive correlations respectively.

The linear regression model followed was $y = b_1 x + b_0$ where y is the dependent variable (either modulus or peak stress), x is the independent variable (density), b_0 is the intercept, and b_1 is the coefficient. The linear regression shows that $R^2 = 0.87, 0.45,$ and 0.16 for pooled, cortical, and cancellous bones respectively.

The power law relationships between ash density and Young's modulus for pooled (cortical and cancellous), cortical and cancellous bones as well as their adjusted coefficients of determination (R^2) are presented in Figure 11, Figure 12 and Figure 13 respectively.. Table 10 below summarizes the linear regression analyses and power-law relationship parameters utilized.

Table 10: Summary of the linear regression analyses and power-law curve fitting between compressive modulus and ash density. The significance level was taken as α = 0.01.

Test Type	Bone Type	Linear regression			Power-law		Parameter estimates	
		R	R^2	P-value	R	R^2	Constant	b1
	Pooled	0.936	0.874	0.000	0.886	0.784	4810.383	1.706
Compression	Cortical	0.692	0.469	0.000	0.723	0.514	4647.771	2.294
	Cancellous	0.415	0.162	0.000	0.432	0.177	2544.519	0.950
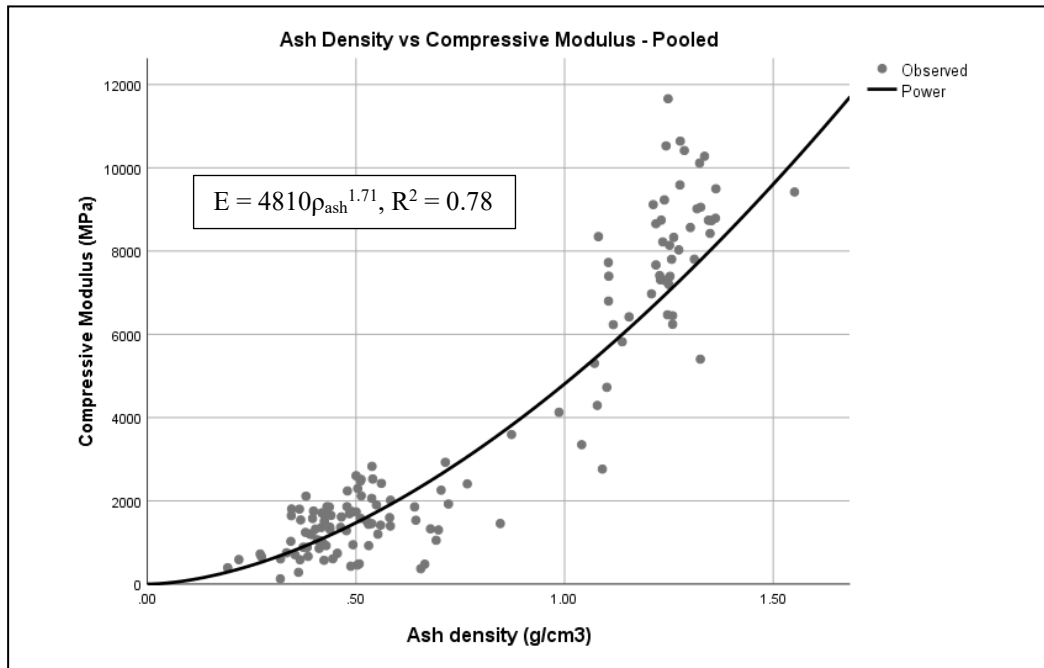
Figure 11: Variation of Compressive Modulus (MPa) with Ash Density (g/cm³) of pooled bones.

Figure 12: Variation of Compressive Modulus (MPa) with Ash Density (g/cm³) of cortical bones.

Figure 13: Variation of Compressive Modulus (MPa) with Ash Density (g/cm³) of cancellous bones.

The compressive peak stress was also assessed with ash density information. The relationships between ash density and compressive peak stress for pooled, cortical and cancellous bones as well as their coefficients of determination (R^2) are presented in Figure 14, Figure 15, and Figure 16 respectively. The power-law relationship yielded a strong positive relationship for pooled bones (R = 0.89, R^2 = 0.80). Cortical bones (R = 0.65, R^2 = 0.41) and Cancellous bones (R = 0.60, R^2 = 0.35) showed medium positive correlations respectively. Table 11 below summarizes the linear regression analyses and power-law relationship parameters utilized.

Table 11: Summary of the linear regression analyses and power-law curve fitting between compressive peak stress and ash density. The significance level was taken as α = 0.01.

Test Type	Bone Type	Linear regression			Power-law		Parameter estimates	
		R	R^2	P-value	R	R^2	Constant	b1
	Pooled	0.921	0.847	0.000	0.894	0.799	65.135	2.617
Compression	Cortical	0.599	0.347	0.000	0.645	0.405	75.942	2.545
	Cancellous	0.584	0.333	0.000	0.596	0.347	44.551	2.154
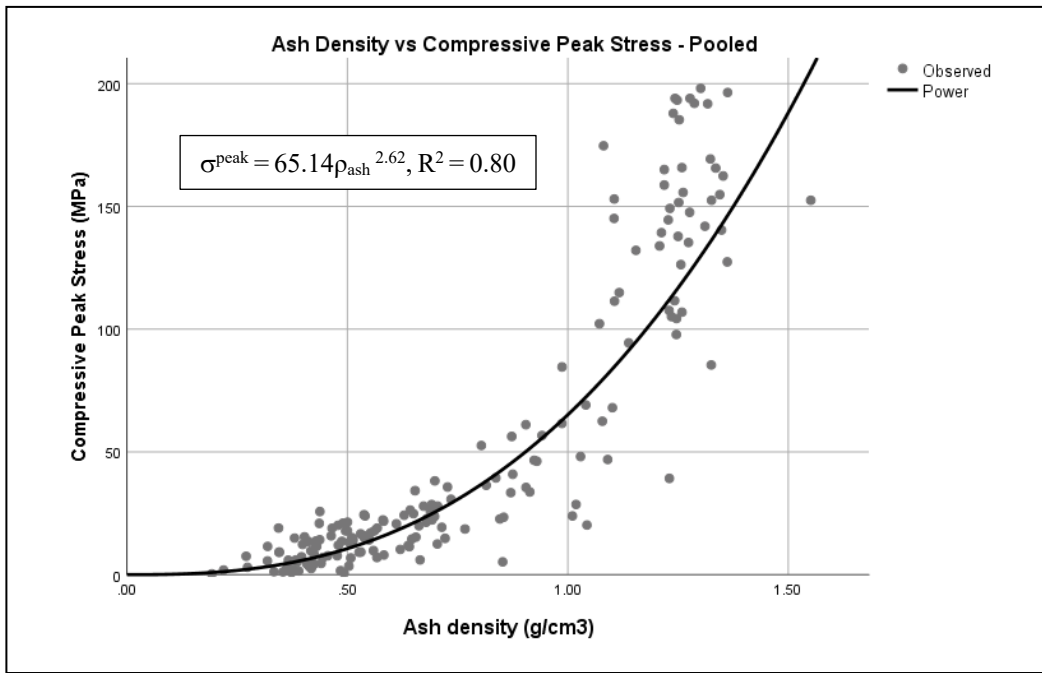
Figure 14: Variation of Compressive Peak Stress (MPa) with Ash Density (g/cm³) of pooled bones.
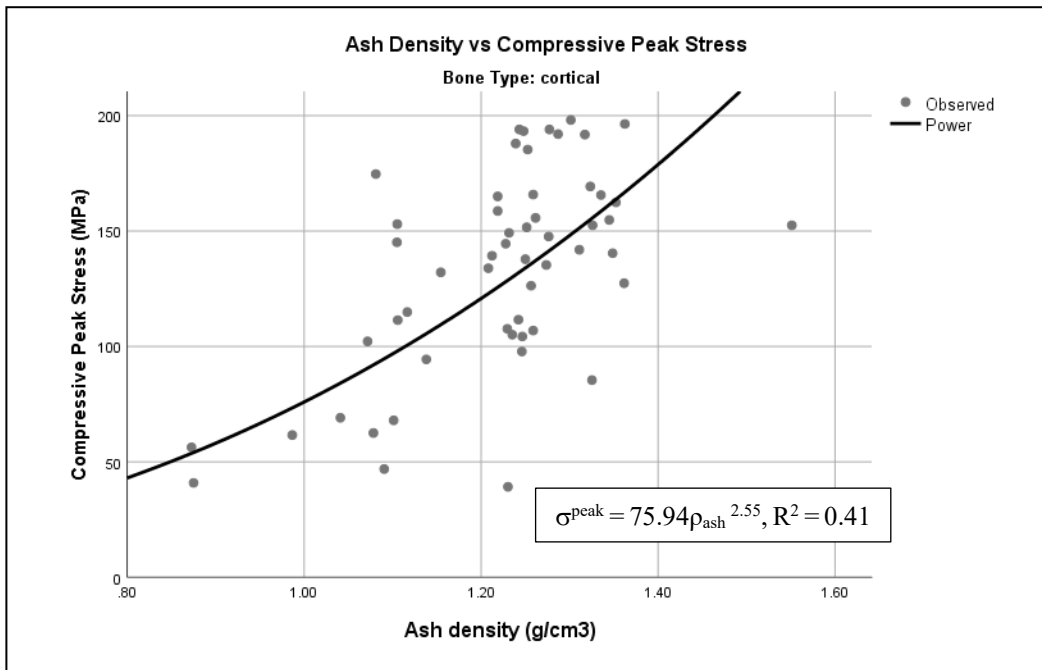
Figure 15: Variation of Compressive Peak Stress (MPa) with Ash Density (g/cm³) of cortical bones.

Figure 16: Variation of Compressive Peak Stress (MPa) with Ash Density (g/cm³) of cancellous bones.

6.3.2 Tension

The properties (Young's modulus, yield stress, break stress, ultimate stress, ultimate strain, and energy to yield) obtained from tension testing are summarized in Table 12 and Table 13 below, including ash density information.

Table 12: Summary of the obtained elastic properties of cancellous bones in tension.

Cancellous		E (MPa)	ρ (g/cm³)	σ^{Yield}(MPa)	σ^{Peak}(MPa)	σ^{Break}(MPa)	Y^{Energy} (Nmm)	ρ_{ash} (g/cm³)
N	Valid	86	90	84	86	83	90	90
	Missing	4	0	6	4	7	0	0
Mean		562.148	1.379	4.891	5.809	3.811	32.286	0.493
SE		44.102	0.012	0.366	0.383	0.287	5.534	0.014
Minimum		42.703	1.029	-0.586[a]	0.000	-0.058[a]	-73.019[a]	0.270
Maximum		2015.658	1.629	22.735	22.700	14.107	252.482	1.227

Missing: the number of specimens that did not produce any output.

Abbreviations: N = sample size, SE = Standard Error of the mean

Y^{Energy} = Energy to yield.

[a] the specimen underwent more compression than tension, thus affecting the machine displayed values.

Table 13: Summary of the obtained elastic properties of cortical bones in tension.

Cortical		E (MPa)	ρ (g/cm³)	σ^{Yield}(MPa)	σ^{Peak}(MPa)	σ^{Break}(MPa)	Y^{Energy} (Nmm)	ρ$_{ash}$ (g/cm³)
N	Valid	48	48	42	47	42	48	48
	Missing	0	0	6	1	6	0	0
Mean		3638.3004	2.059	27.230	30.535	27.034	282.247	1.237
SE		130.639	0.019	1.994	1.863	1.887	98.374	0.019
Minimum		692.520	1.680	6.595	7.300	7.303	-124.124[a]	0.815
Maximum		5156.799	2.246	52.696	59.200	55.025	3373.663	1.390

Missing: the number of specimens that did not produce any output.

Abbreviations: N = sample size, SD = Standard Deviation, SE = Standard Error of the mean

Y^{Energy} = Energy to yield.

[a] the specimen underwent more compression than tension, thus affecting the machine displayed values.

The average Young's modulus of cortical bone in tension is almost six times greater than that of cancellous bone in this work. The average ultimate and break strength of cortical bone are close to six times that of cancellous bone. The range for ash density, including cancellous and cortical bone, is from 0.270g/cm³ to 1.390g/cm³.

The relationships between ash density and Young's modulus for pooled, cortical and cancellous bones as well as their coefficients of determination are presented in Figure 17, Figure 18, and Figure 19 respectively. The power-law relationship showed a strong positive relationship (R = 0.88, R^2 = 0.78) between ash density and Young's modulus. Cortical bones (R = 0.68, R^2 = 0.45) and Cancellous bones (R = 0.50, R^2 = 0.24) showed medium and low positive relationships. Table 14 below summarizes the linear regression analyses and power-law relationship parameters utilized.

Table 14: Summary of the linear regression analyses and power-law curve fitting between tensile modulus and ash density. The significance level was taken as α = 0.01.

Test Type	Bone Type	Linear regression			Power-law		Parameter estimates	
		R	R^2	P-value	R	R^2	Constant	b1
Tension	Pooled	0.963	0.927	0.000	0.881	0.775	2189.756	2.174
	Cortical	0.668	0.433	0.000	0.677	0.446	2479.402	1.805
	Cancellous	0.451	0.194	0.000	0.499	0.240	1633.480	1.815
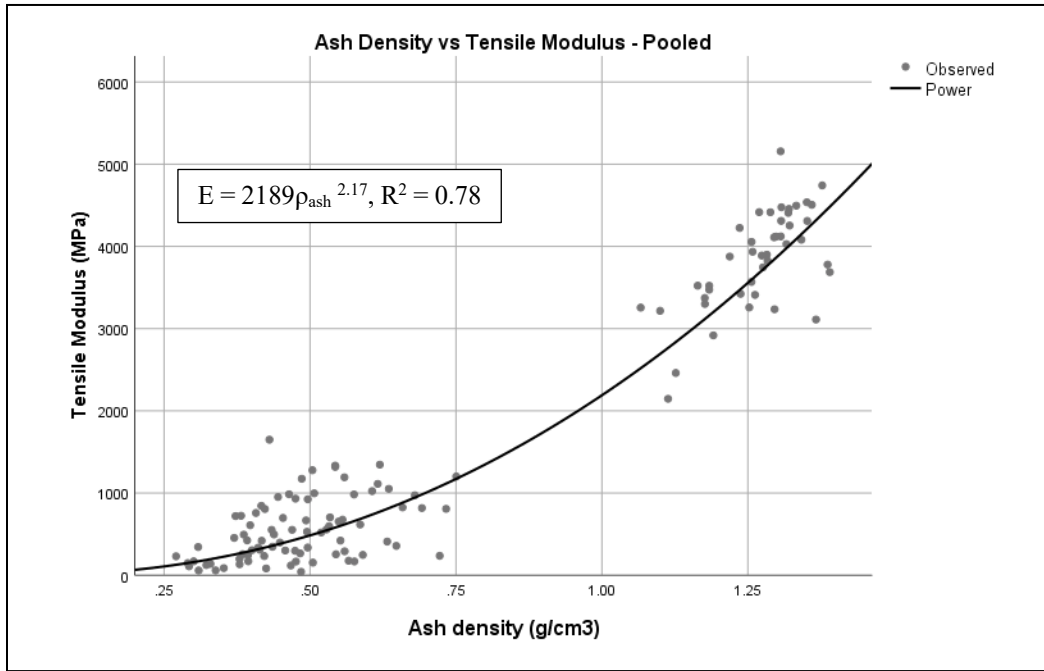
Figure 17: Variation of tensile Modulus (MPa) with Ash Density (g/cm³) of pooled bones.
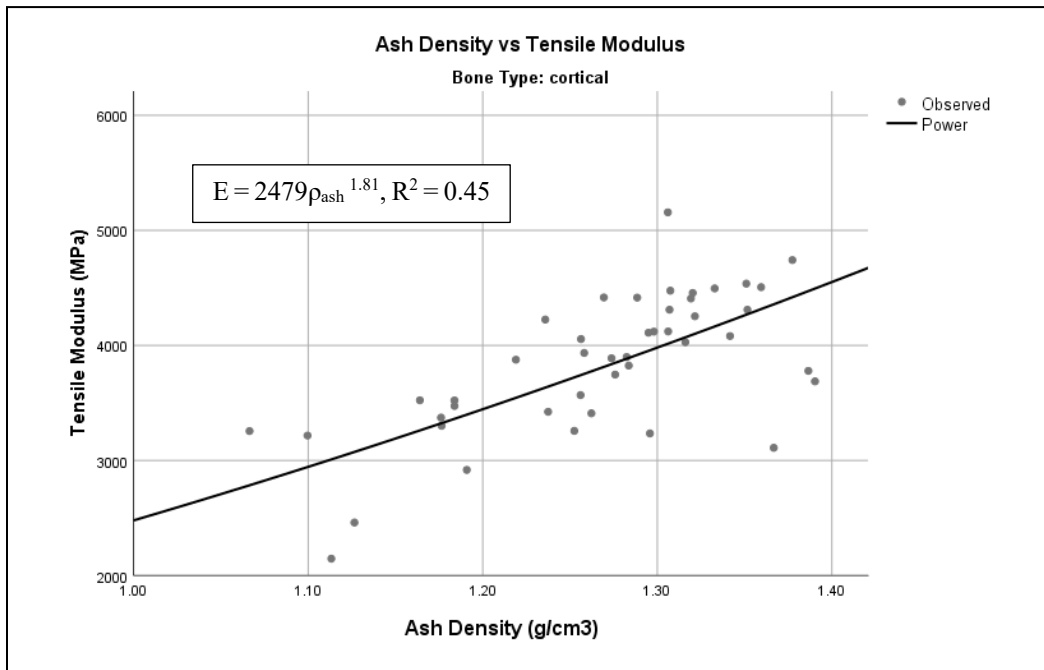
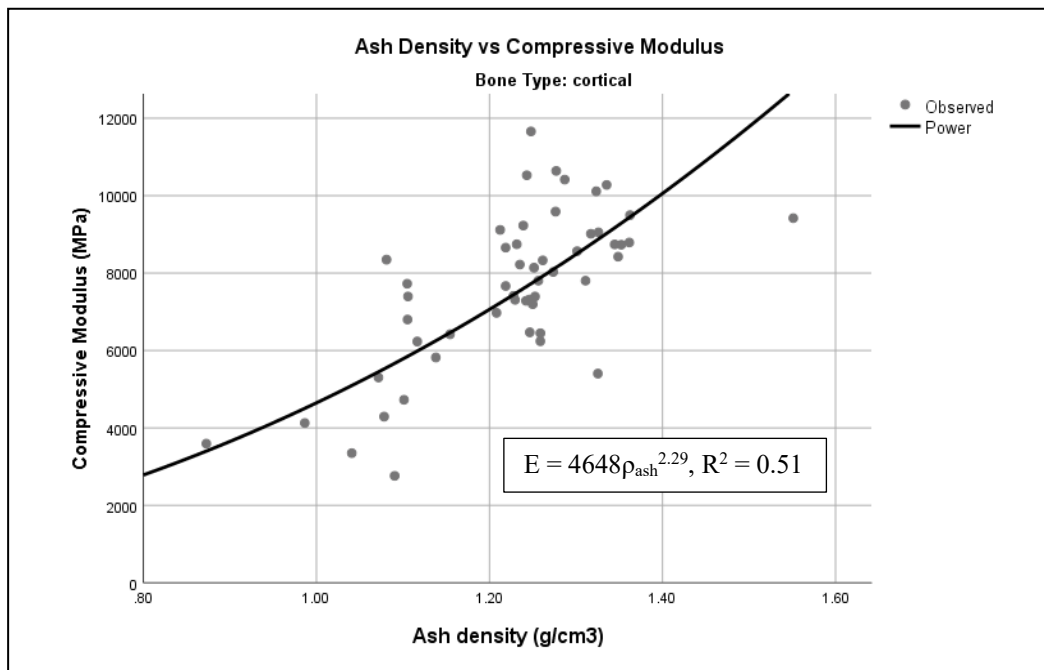*Figure 18: Variation of tensile Modulus (MPa) with Ash Density (g/cm³) of cortical bones.*

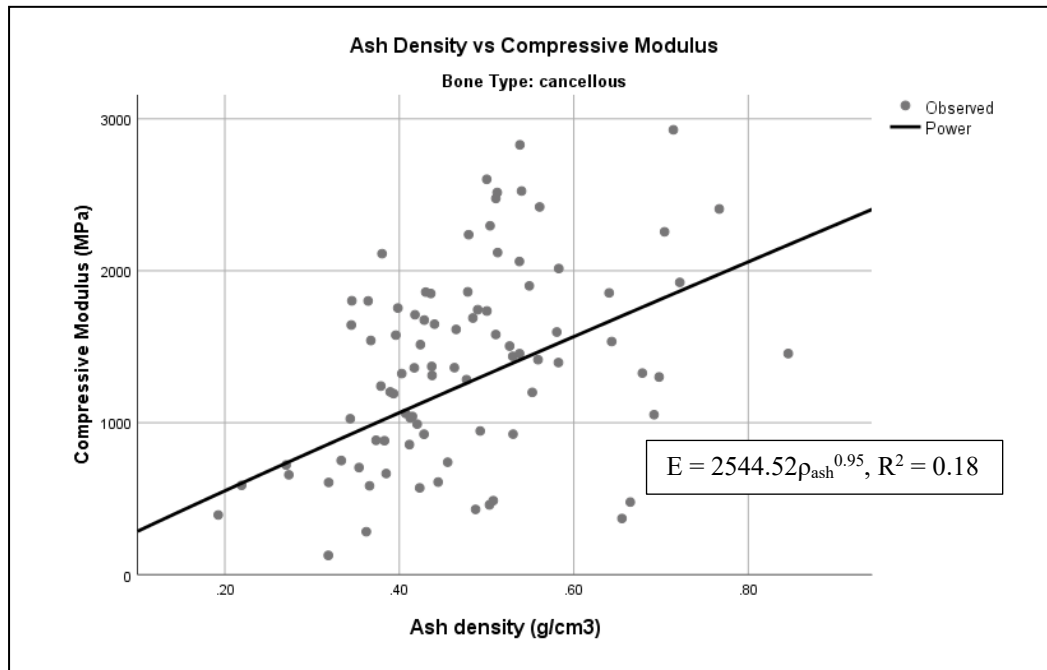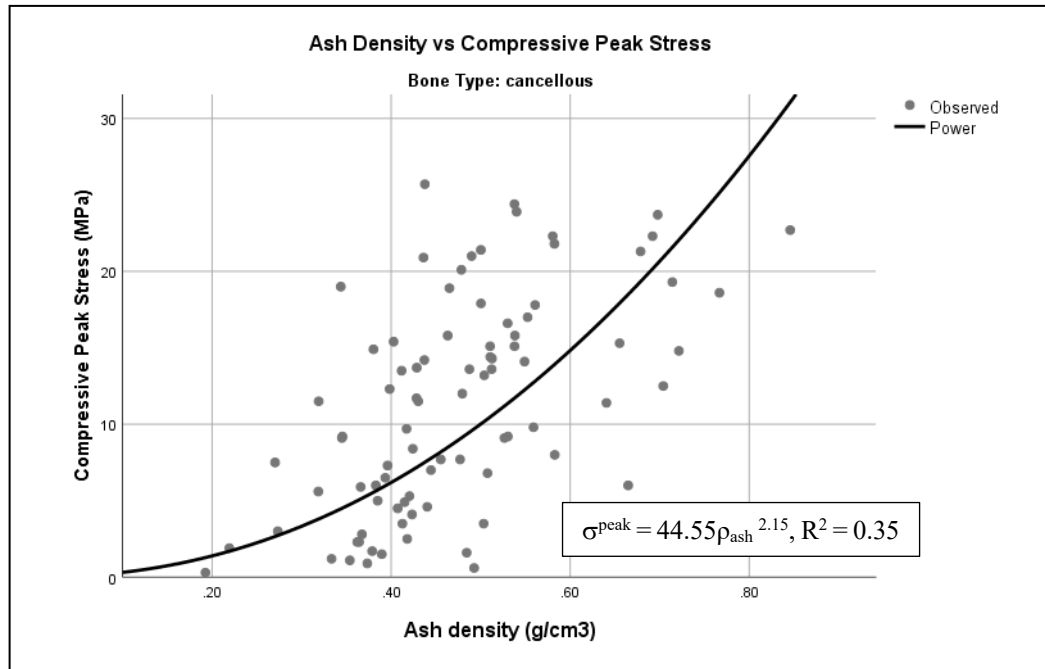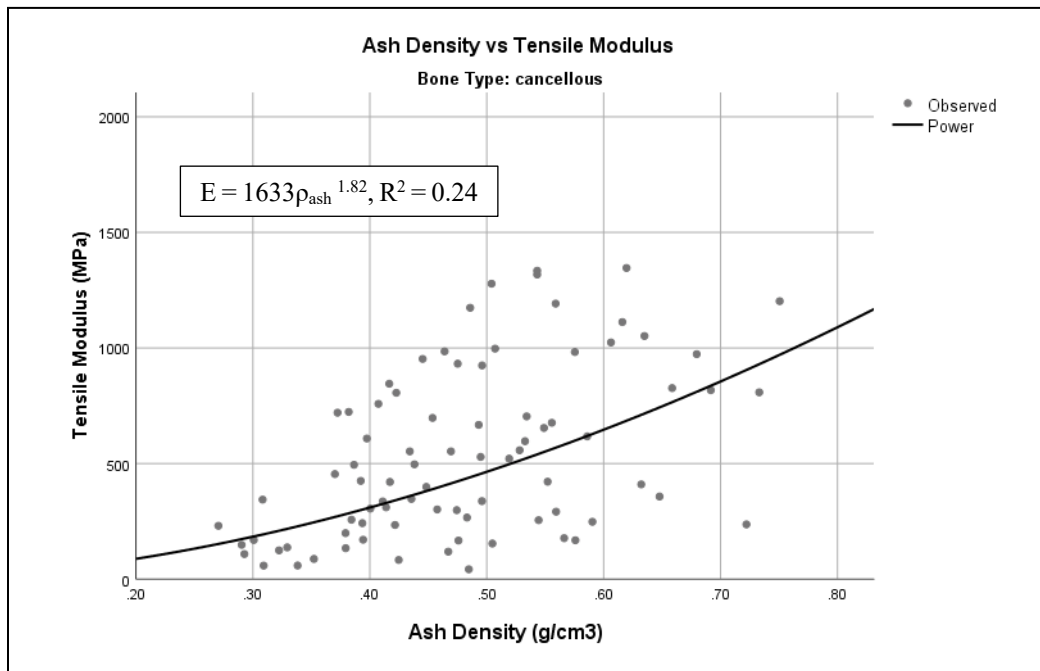*Figure 19: Variation of tensile Modulus (MPa) with Ash Density (g/cm³) of cancellous bones.*

The tensile peak stress was also assessed with ash density information. The relationships between ash density and tensile peak stress for pooled, cortical and cancellous bones as well as their coefficients of determination are presented in Figure 20, Figure 21, and Figure 22 respectively. The power-law relationships indicate R^2 values of 0.63, 0.02, and 0.20 for Pooled, Cancellous and Cortical bones, respectively. Similarly, the linear regression relationships indicate R^2 values of 0.67, 0.02, and 0.50 for the bone types. Table 15 below summarizes the linear regression analyses and power-law relationship parameters utilized.

Table 15: Summary of the linear regression analyses and power-law curve fitting between tensile peak stress and ash density. The significance level was taken as α = 0.01.

Test Type	Bone Type	Linear regression			Power-law		Parameter estimates	
		R	R^2	P-value	R	R^2	Constant	b1
	Pooled	0.821	0.671	0.000	0.796	0.630	18.251	1.860
Tension	Cortical	0.201	0.017	0.195	0.200	0.016	40.363	-1.463
	Cancellous	0.713	0.502	0.000	0.466	0.207	18.016	1.853
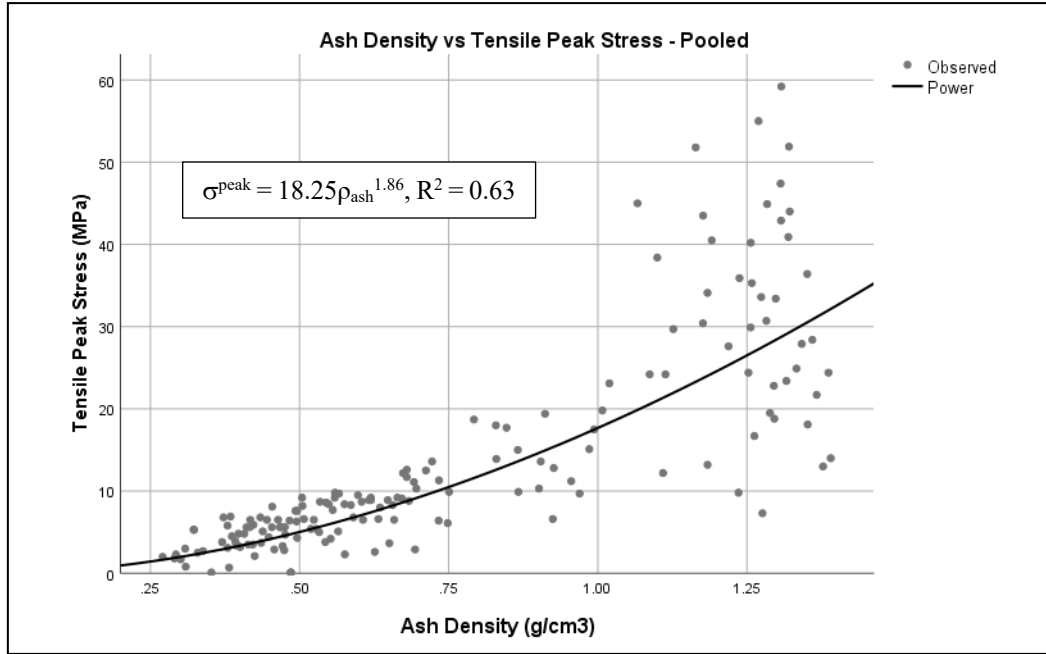
Figure 20: Variation of tensile Peak Stress (MPa) with Ash Density (g/cm³) of pooled bones.
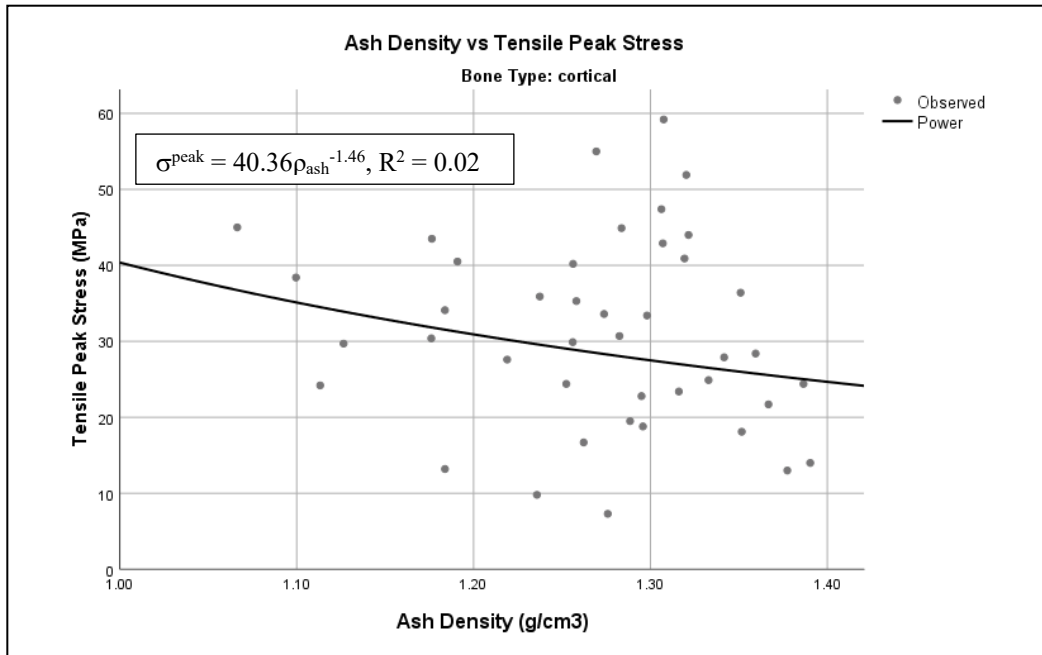
Figure 21: Variation of tensile Peak Stress (MPa) with Ash Density (g/cm³) of cortical bones.
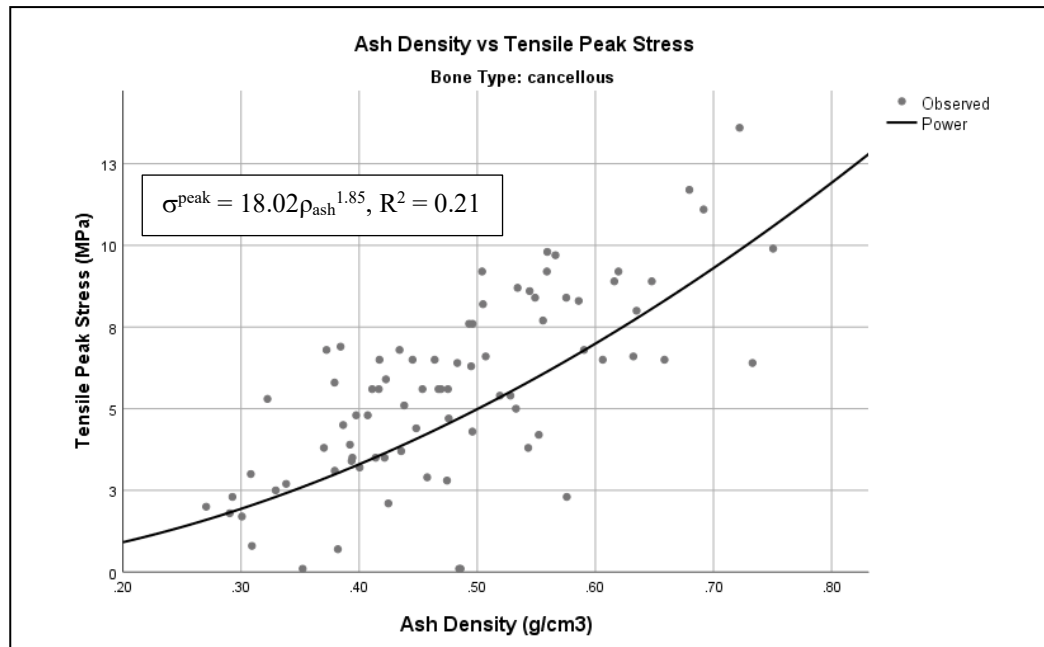
Figure 22: Variation of tensile Peak Stress (MPa) with Ash Density (g/cm³) of cancellous bones.

6.3.3   Effect of Organic Content – Compression

The relationships between organic density and Young's modulus for pooled, cortical and cancellous bones as well as their coefficients of determination are presented in Figure 23, Figure 24, and Figure 25. Organic density information itself predictably exhibited low influence on the mechanical properties, as is evident in the R^2 values in the summary of empirical relationship parameters shown in Table 16 below. For cortical and cancellous bones, the effect of organic density alone on the mechanical properties of bone is not statistically significant ($p > 0.05$) compared with the ash density relationship with modulus ($p < 0.05$). However, the pooled bones showed statistical significance with R^2 values of 0.54 (power-law) and 0.55 (linear regression).

Table 16: *Summary of the linear regression analyses and power-law curve fitting between compressive modulus and organic density. The significance level was taken as α = 0.01.*

Test Type	Bone Type	Linear regression			Power-law		Parameter estimates	
		R	R^2	P-value	R	R^2	Constant	b1
Compression	Pooled	0.744	0.550	0.000	0.737	0.540	251.157	-5.307
	Cortical	0.183	0.033	0.191	0.153	0.004	4633.703	-0.785
	Cancellous	0.196	0.038	0.074	0.170	0.017	876.162	-1.015
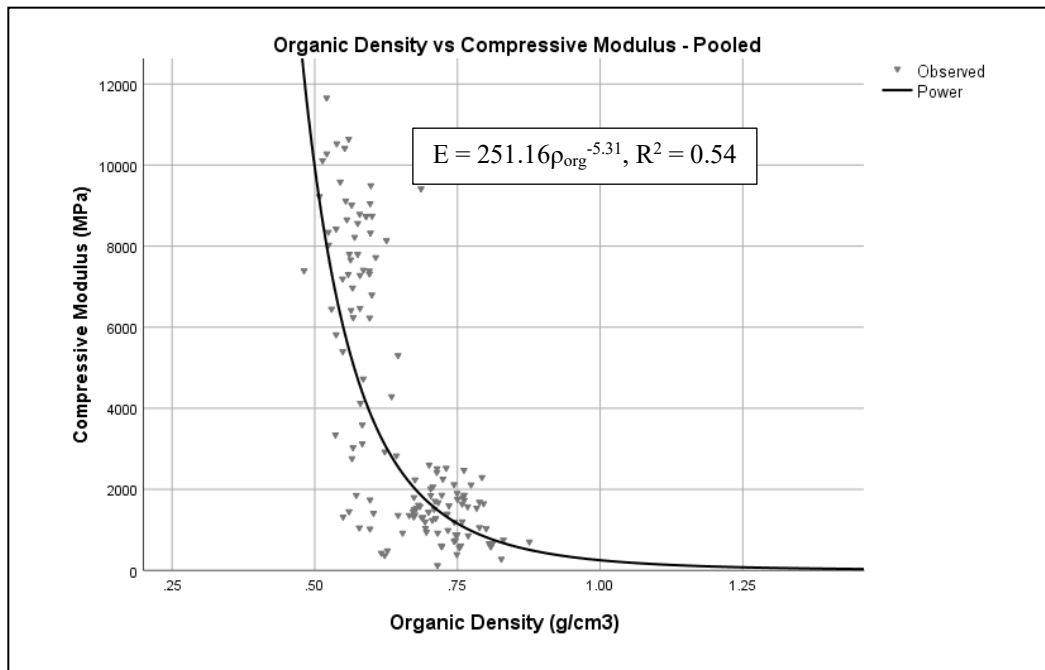
Figure 23: *Variation of compressive Modulus (MPa) with Organic Density (g/cm³) of pooled bones.*

Figure 24: Variation of compressive Modulus (MPa) with Organic Density (g/cm³) of cortical bones.

Figure 25: Variation of compressive Modulus (MPa) with Organic Density (g/cm³) of cancellous bones.

The density ratio (ash density/organic density) as the determinant of the compressive modulus was also assessed. Table 17 below summarizes the linear regression analyses and power-law relationship parameters utilized. The power-law relationships indicate a strong positive relationship (R = 0.89, R^2 = 0.79) for Pooled bones, and a medium positive relationship for Cortical bones (R = 0.89, R^2 = 0.50). These relationships are shown in Figure 26, Figure 27, and Figure 28.

Table 17: Summary of the linear regression analyses and power-law curve fitting between compressive modulus and density ratio. The significance level was taken as α = 0.01.

Test Type	Bone Type	Linear regression			Power-law		Parameter estimates	
		R	R^2	P-value	R	R^2	Constant	b1
	Pooled	0.939	0.880	0.000	0.890	0.791	3357.241	1.565
Compression	Cortical	0.712	0.497	0.000	0.715	0.502	2531.365	2.301
	Cancellous	0.406	0.155	0.000	0.453	0.197	2274.283	1.002
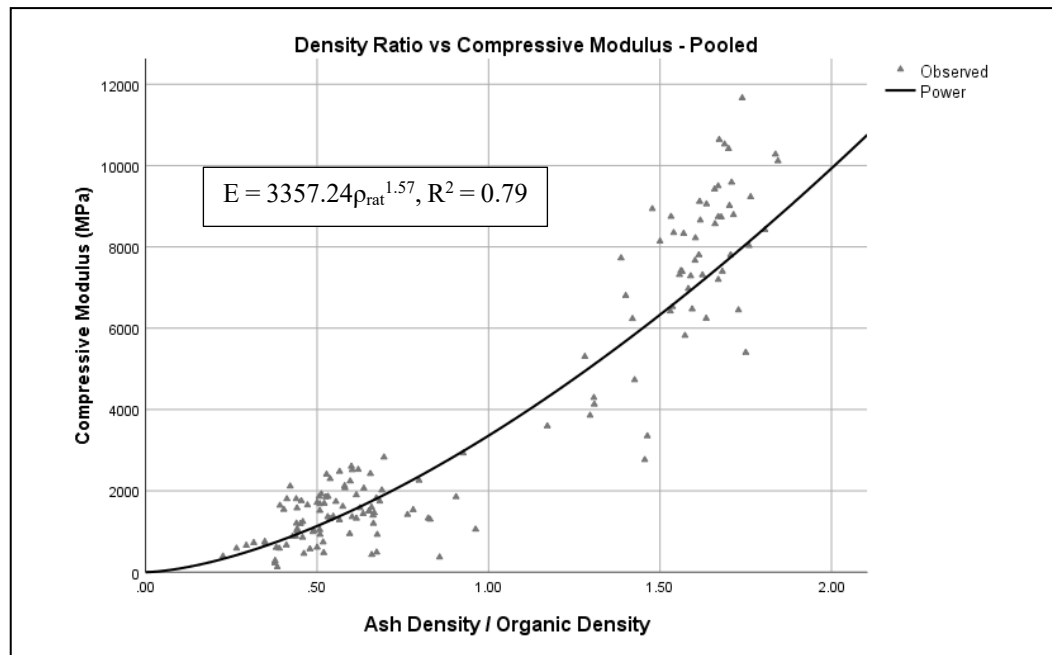
Figure 26: Variation of compressive Modulus (MPa) with Ash Density/Organic Density of pooled bones.

Figure 27: Variation of compressive Modulus (MPa) with Ash Density/Organic Density of cortical bones.

Figure 28: Variation of compressive Modulus (MPa) with Ash Density/Organic Density of cancellous bones.

The variation of ash/organic density ratio with peak stress was also obtained. Table 18 below summarizes the linear regression analyses and power-law relationship parameters utilized. The power-law relationship indicates a strong positive relationship ($R = 0.92$, $R^2 = 0.85$) for pooled bones. Cortical bones ($R = 0.74$, $R^2 = 0.54$) and cancellous bones ($R = 0.66$, $R^2 = 0.43$). The linear regression also showed a strong positive relationship ($R = 0.93$, $R^2 = 0.86$) for pooled bones. The variations for pooled, cortical and cancellous bones can be seen in Figure 29, Figure 30, and Figure 31.

Table 18: Summary of the linear regression analyses and power-law curve fitting between compressive peak stress and density ratio. The significance level was taken as α = 0.01.

Test Type	Bone Type	Linear regression			Power-law		Parameter estimates	
		R	R^2	P-value	R	R^2	Constant	b1
Compression	Pooled	0.930	0.864	0.000	0.923	0.851	39.886	2.463
	Cortical	0.682	0.455	0.000	0.740	0.539	30.315	3.094
	Cancellous	0.622	0.379	0.000	0.657	0.426	36.134	2.317
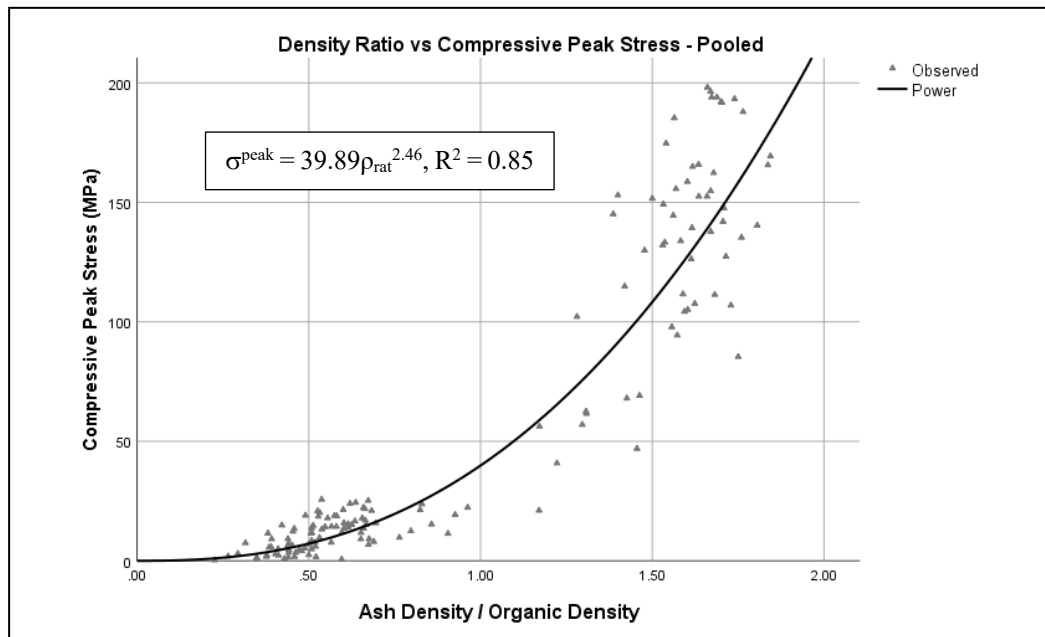
Figure 29: Variation of compressive Peak Stress (MPa) with Ash Density/Organic Density of pooled bones.
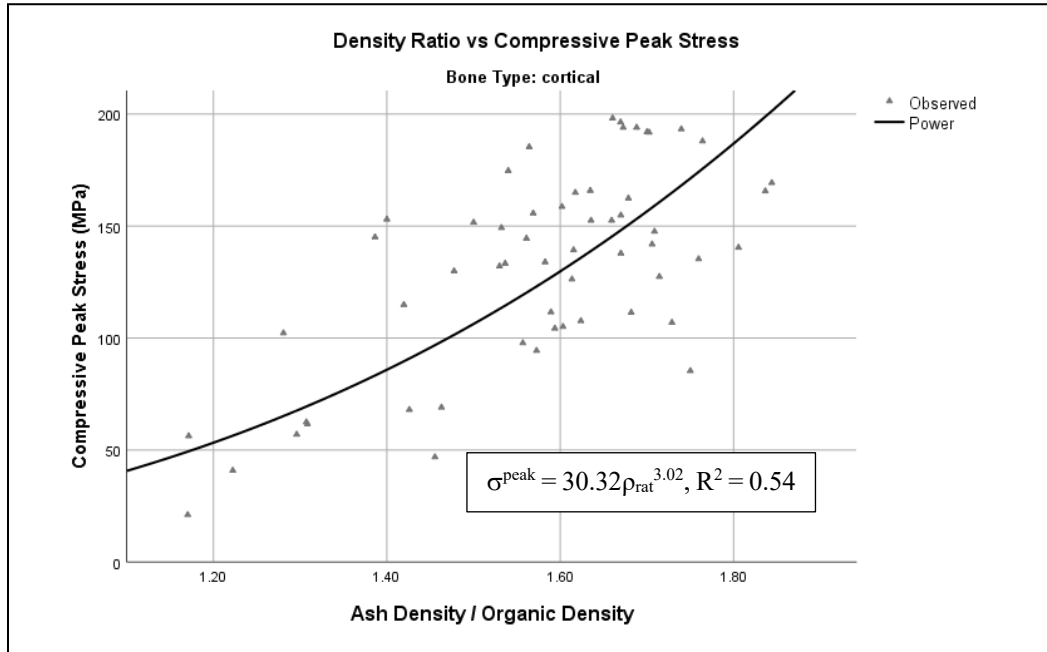
Figure 30: Variation of compressive Peak Stress (MPa) with Ash Density/Organic Density of cortical bones.

Figure 31: Variation of compressive Peak Stress (MPa) with Ash Density/Organic Density of cancellous bones.

6.3.4   Effect of Organic Content – Tension

The relationships between organic density and tensile Young's modulus for pooled (corti-cal and cancellous), cortical and cancellous bones as well as their correlation are presented in Figure 32, Figure 33, and Figure 34 below. As illustrated in the compression section of organic content effect (Section 6.3.3), organic density information itself predictably showed low influence on the mechanical properties as is evident in the R^2 values in the summary of empirical relationship parameters shown in Table 19 below. For cortical bones, the effect of organic density alone on the mechanical properties of bone is not sta-tistically significant ($p > 0.05$) compared with ash density relationship with modulus ($p < 0.05$). Both the power-law and linear regression models indicate a correlation (R) of 0.71 and a coefficient of determination (R^2) of 0.50.

Table 19: Summary of the linear regression analyses and power-law curve fitting between tensile modulus and organic density. The significance level was taken as α = 0.01.

| Test Type	Bone Type	Linear regression			Power-law		Parameter estimates	
		R	R^2	P-value	R	R^2	Constant	b1
Tension	Pooled	0.709	0.498	0.000	0.708	0.497	25.674	-8.221
	Cortical	0.070	0.005	0.661	0.039	0.002	3530.996	-0.164
	Cancellous	0.305	0.082	0.005	0.317	0.089	138.632	-2.900
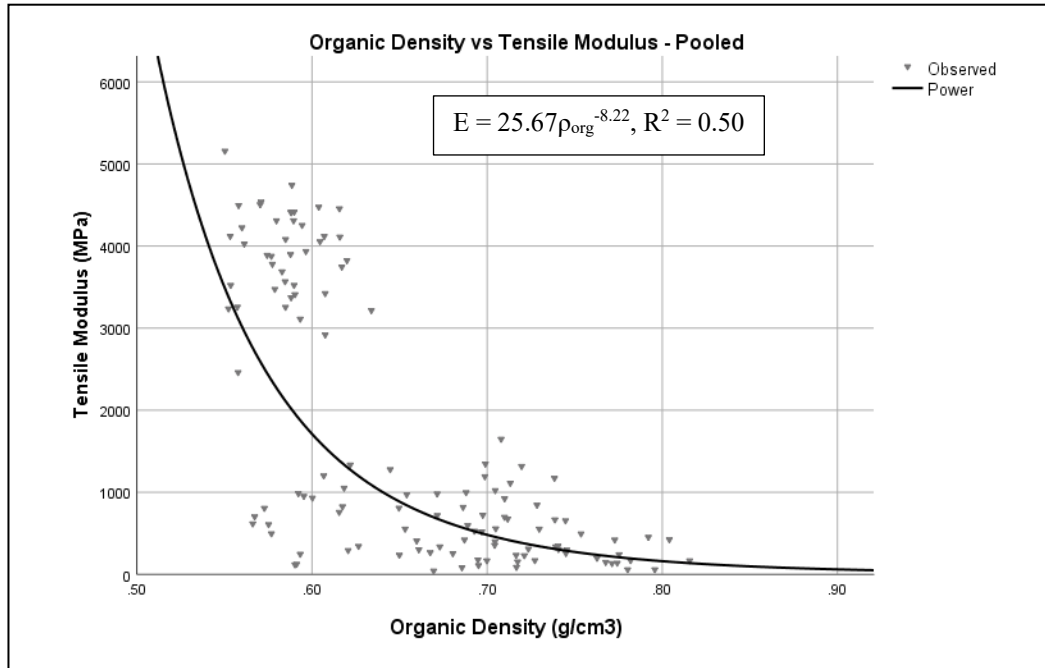
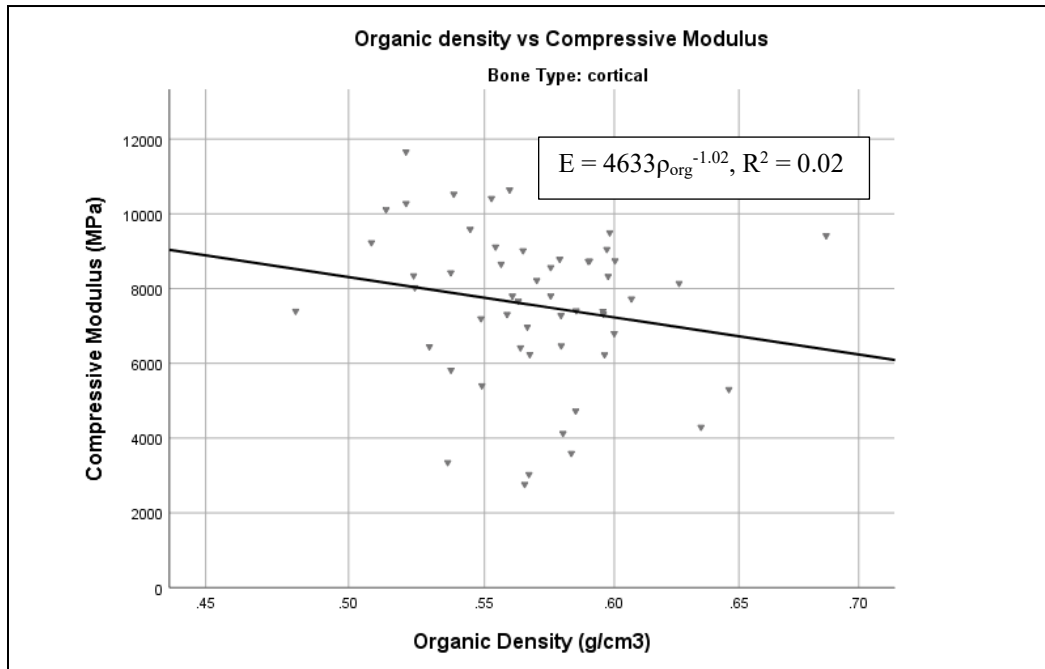*Figure 32: Variation of tensile Modulus (MPa) with Organic Density (g/cm³) of pooled bones.*
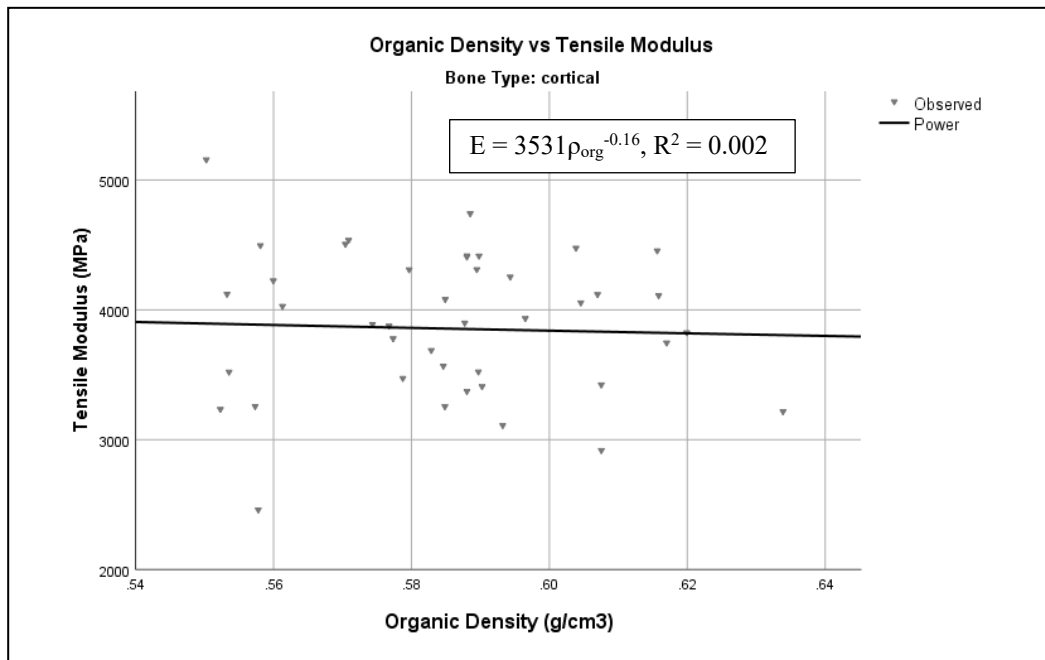
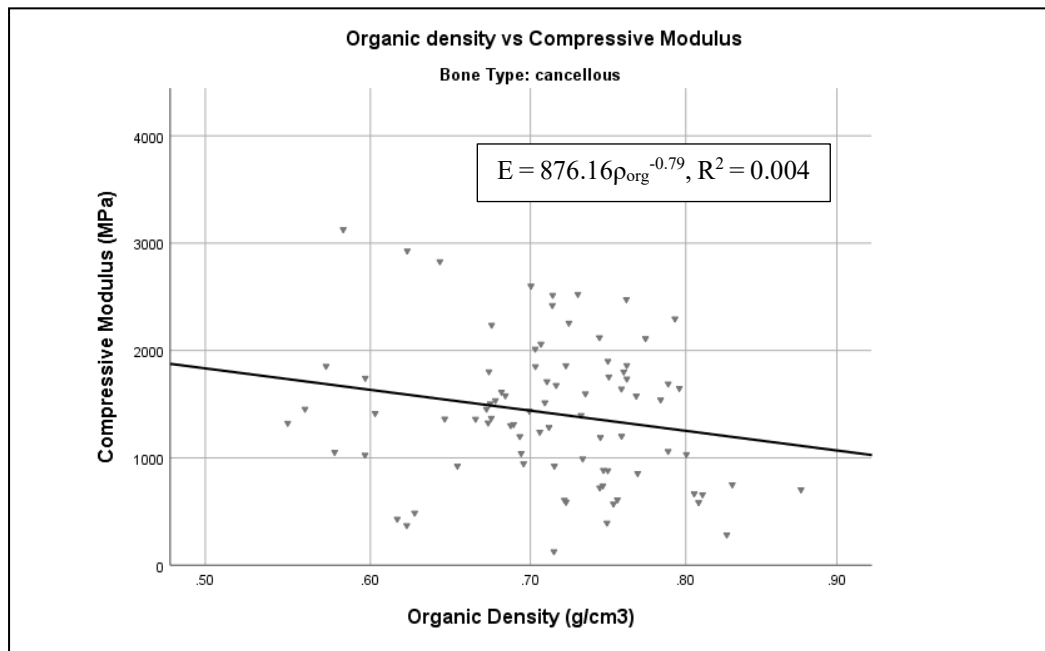*Figure 33: Variation of tensile Modulus (MPa) with Organic Density (g/cm³) of cortical bones.*
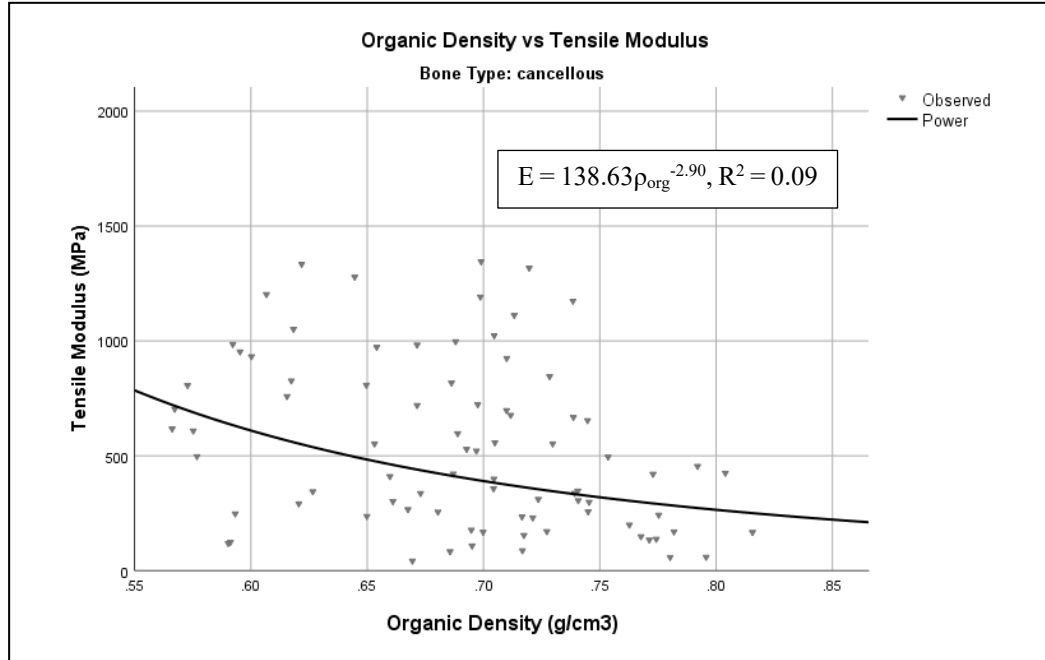
Figure 34: Variation of tensile Modulus (MPa) with Organic Density (g/cm³) of cancellous bones.

The variation of tensile modulus with ash/organic density ratio was also assessed. Table 20 below summarizes the linear regression analyses and power-law relationship parameters utilized. The power-law relationships indicate R^2 = 0.78, 0.24, and 0.27 for Pooled, Cortical, and Cancellous bones respectively. The linear regression yielded an R^2 of 0.92 for pooled bones. Figure 35, Figure 36, and Figure 37 show relationships that explore the ratio of the ash density to the organic density.

Table 20: Summary of the linear regression analyses and power-law curve fitting between tensile modulus and density ratio. The significance level was taken as α = 0.01.

| Test Type	Bone Type	Linear regression			Power-law		Parameter estimates	
		R	R^2	P-value	R	R^2	Constant	b1
	Pooled	0.961	0.923	0.000	0.884	0.780	863.368	1.869
Tension	Cortical	0.522	0.255	0.000	0.492	0.242	1676.007	1.059
	Cancellous	0.465	0.207	0.000	0.522	0.273	758.255	1.587
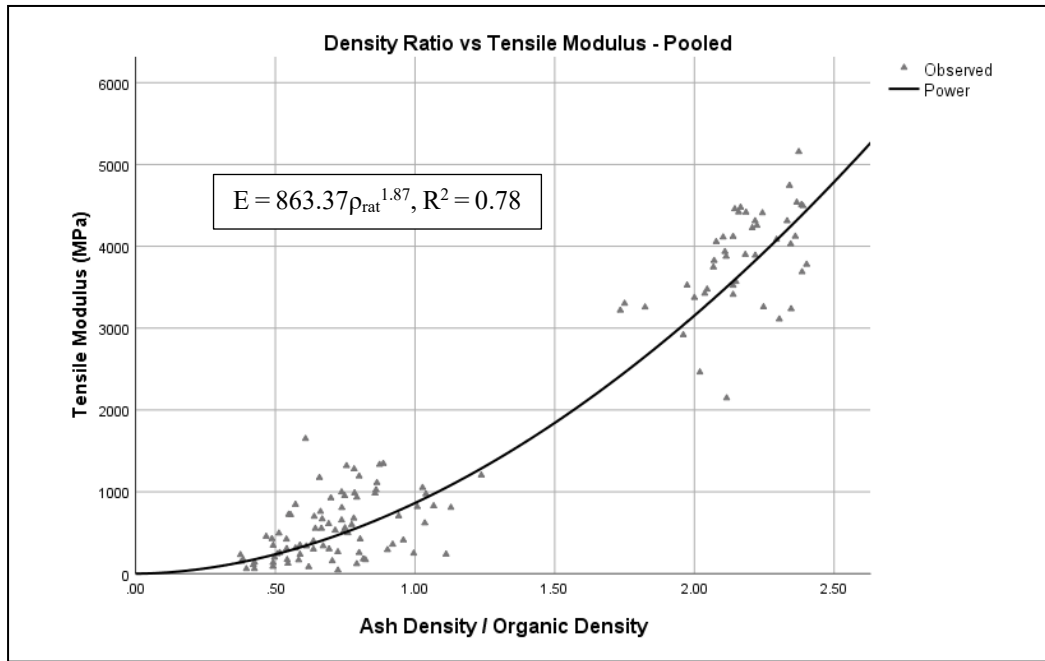
Figure 35: Variation of tensile Modulus (MPa) with Ash Density/Organic Density of pooled bones.
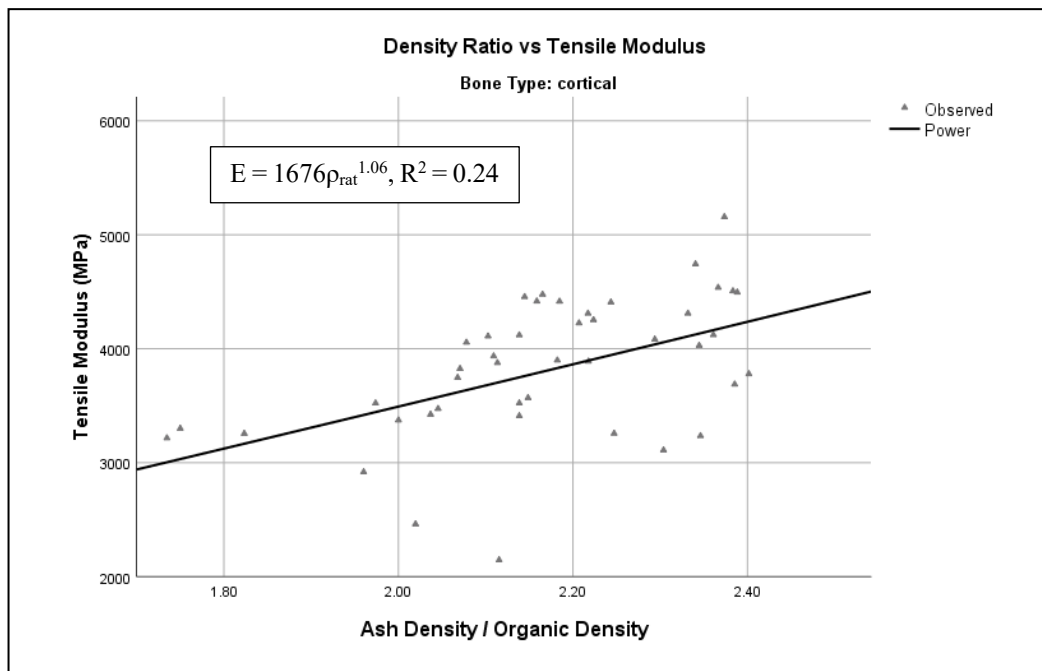
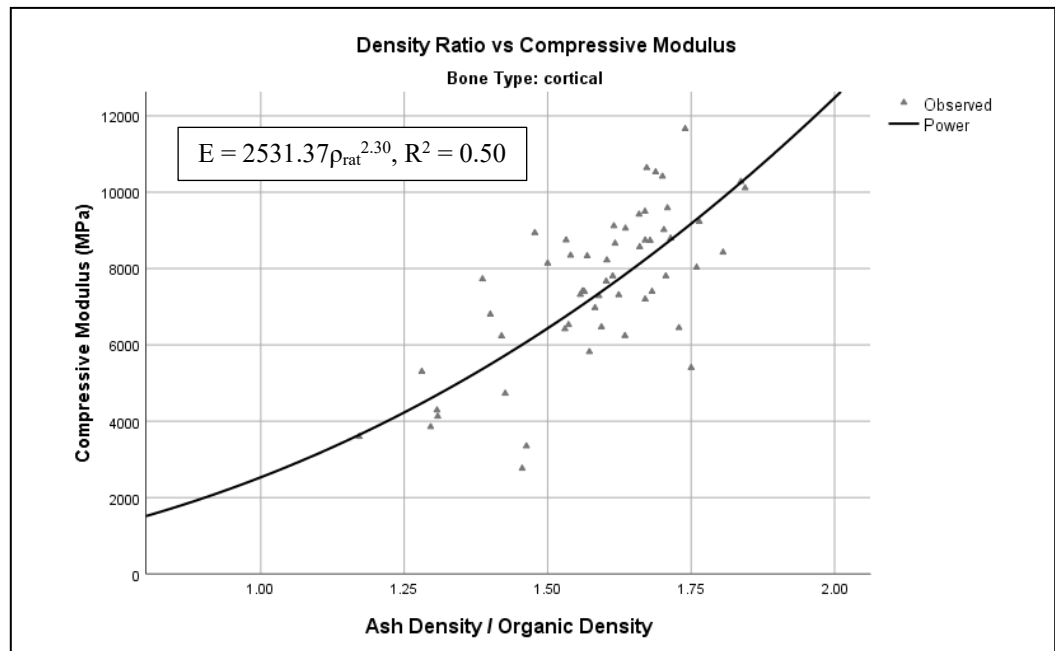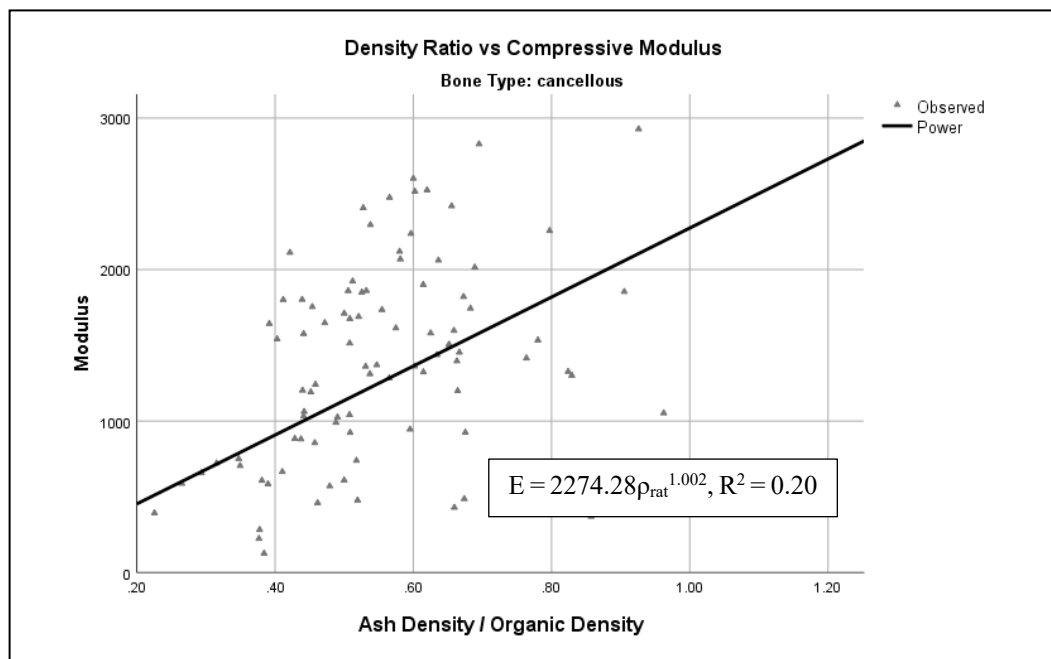*Figure 36: Variation of tensile Modulus (MPa) with Ash Density/Organic Density of cortical bones.*
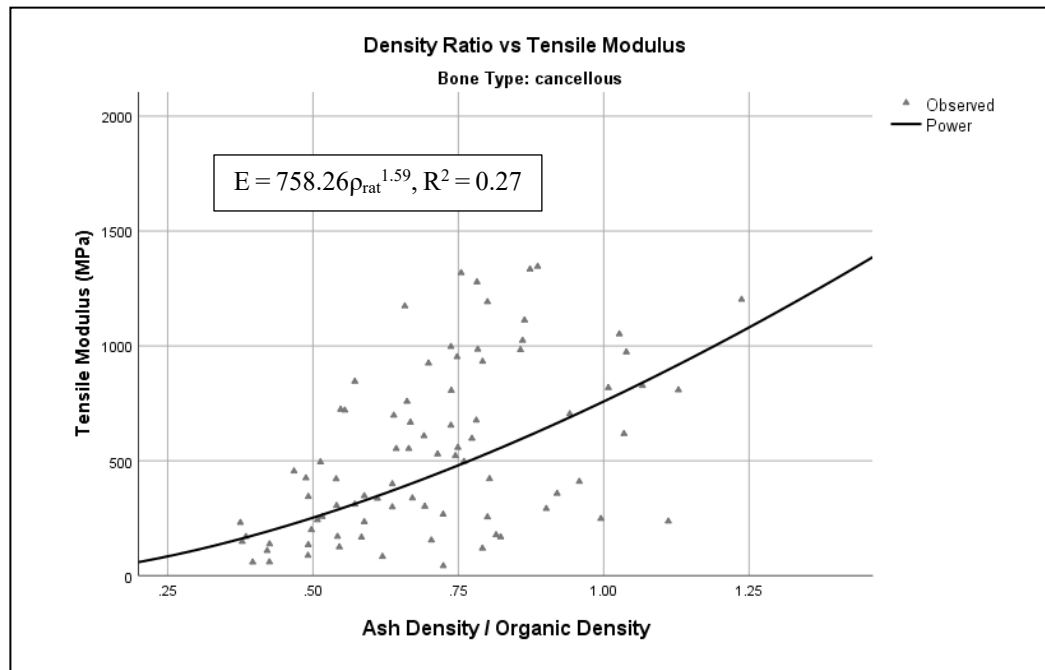
Figure 37: Variation of tensile Modulus (MPa) with Ash Density/Organic Density of cancellous bones.

The variation of tensile peak stress with the ash/organic density ratio was also assessed. Table 21 below summarizes the linear regression analyses and power-law relationship parameters obtained. The power-law relationships indicate an $R^2 = 0.63$ for pooled bones and $R^2 = 0.23$ for cancellous bones. The linear regression yielded an $R^2 = 0.69$ for pooled bones and $R^2 = 0.51$ for cancellous bones. The variations for pooled, cortical and cancellous bones can be seen in Figure 38, Figure 39, and Figure 40. The density ratio relationships showed stronger correlations than inorganic-mechanical property relationships. For pooled bones, there was a 3% increase in correlation (from $R^2 = 0.671$ to 0.689). For cancellous bones, there was a 9% increase in correlation (from $R^2 = 0.502$ to 0.510). Cortical bones did not meet the required significance levels of $p < 0.05$. For a summary of correlation differences, please see Section 6.3.5.

Table 21: Summary of the linear regression analyses and power-law curve fitting between tensile peak stress and density ratio. The significance level was taken as α = 0.01.

Test Type	Bone Type	Linear regression			Power-law		Parameter estimates	
		R	R^2	P-value	R	R^2	Constant	b1
Tension	Pooled	0.821	0.689	0.000	0.798	0.634	8.243	1.600
	Cortical	0.336	0.091	0.028	0.295	0.064	111.627	-1.770
	Cancellous	0.718	0.510	0.000	0.484	0.225	8.216	1.613
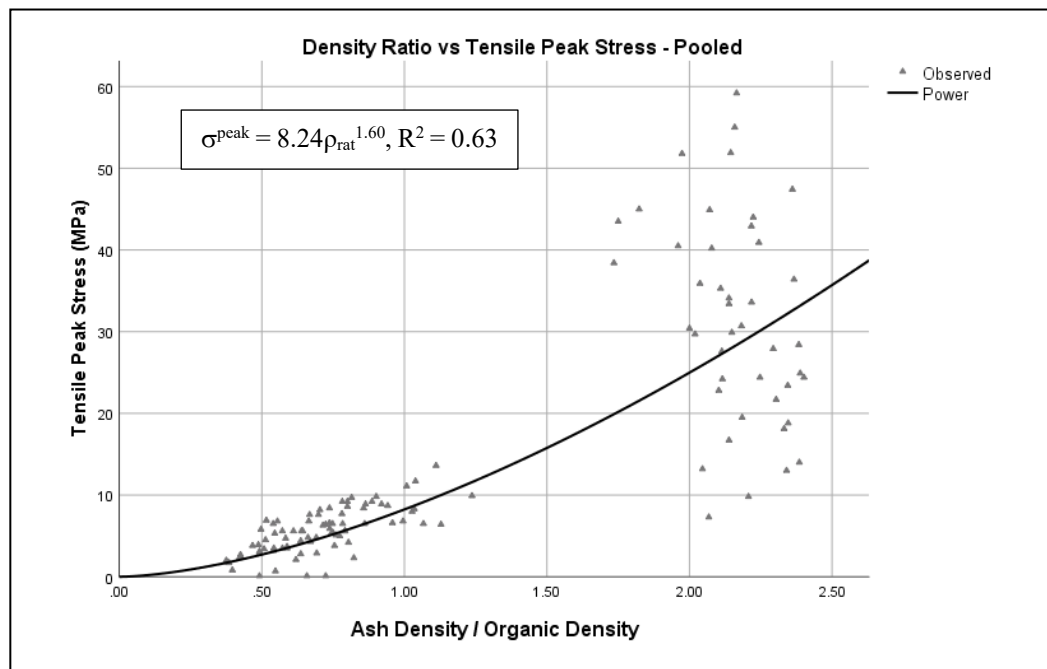
Figure 38: Variation of tensile Peak Stress (MPa) with Ash Density/Organic Density of pooled bones.

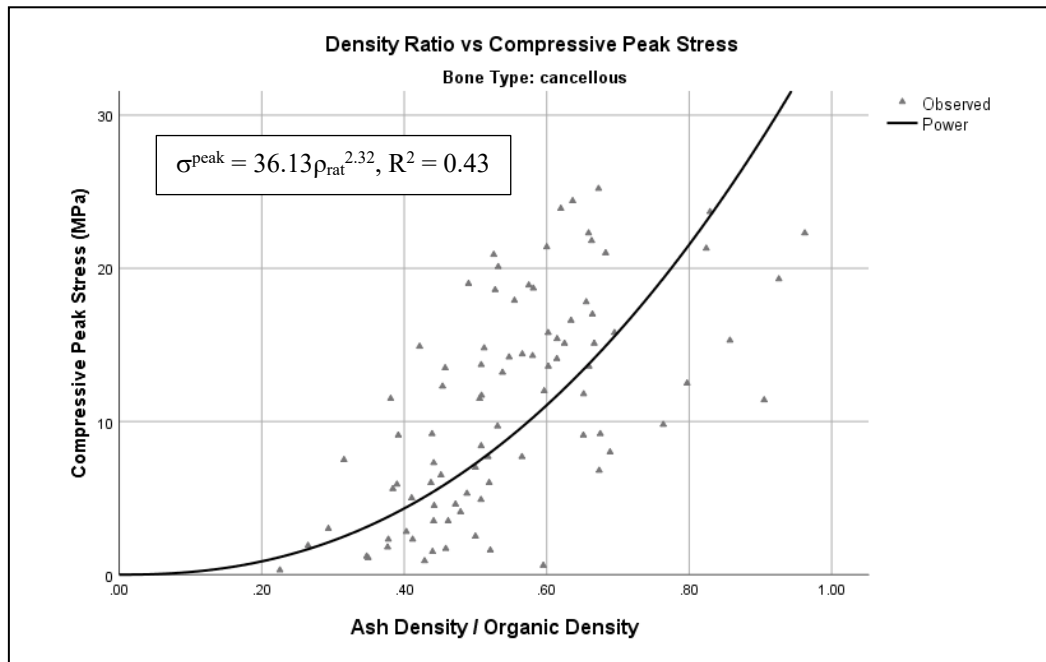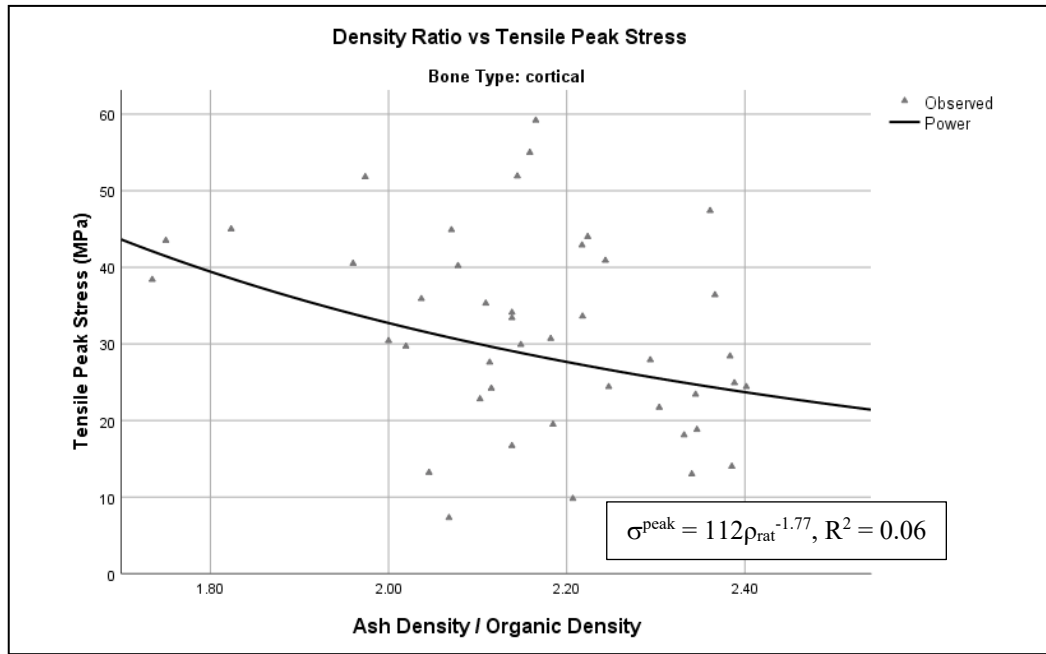*Figure 39: Variation of tensile Peak Stress (MPa) with Ash Density/Organic Density of cortical bones.*
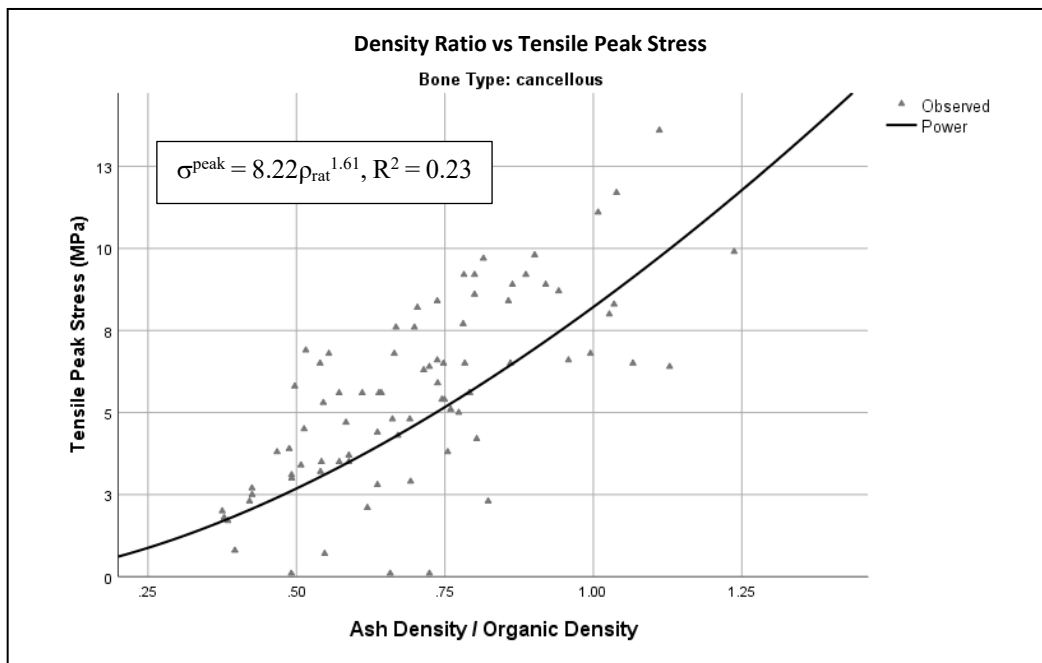
Figure 40: Variation of tensile Peak Stress (MPa) with Ash Density/Organic Density of cancellous bones.

6.3.5   Comparison of Density-Modulus Relationships

A comparison of the *density-modulus* and *density-peak stress* relationships in compression

and tension shows that the mechanical properties (Modulus and Peak Stress) had stronger

correlation with density ratio than with mineral density. This observation was assessed by

exploring the percentage difference in R^2 between the density ratio results and ash density

results. The percentage difference was calculated as $\left(\frac{R^2_{density\ ratio} - R^2_{ash\ density}}{R^2_{ash\ density}}\right) \times 100\%$. A

summary of these differences is shown in Table 22 below.

Table 22: Summary of the percentage differences in R^2 between the density-mechanical property variations examined. Bracketed values represent a decrease in R^2 values.

Test Type	Relationship	Bone Type	R² Difference (Percentage)	
			Power-Law	**Linear Regression**
Compression	Density-Modulus	Pooled	0.89%	0.69%
		Cortical	(2.33%)	5.97%
		Cancellous	11.30%	(4.32%)
	Density-Peak Stress	Pooled	6.5%	2.01%
		Cortical	33.09%	31.12%
		Cancellous	22.77%	13.80%
Tension	Density-Modulus	Pooled	0.65%	0.43%
		Cortical	(84.30%)	(41.11%)
		Cancellous	13.75%	6.70%
	Density-Peak Stress	Pooled	0.63%	2.61%
		Cortical[1]	-	-
		Cancellous	8.70%	1.60%

[1] Cortical bone did not meet the required significance levels of $p < 0.05$

6.4   Discussion

The aim of this research was the study of bone inorganic-organic composition on its mechanical properties. Experimental protocols were improved to aid in the accomplishment of this goal. The protocols were improved based on existing protocols in literature. Of particular interest was the preservation of the moisture of the specimens to be tested. Linde and Sorensen [102] examined different storage methods and found that the freezing of wet specimens has the least and minimal impact on mechanical properties. The existing body of work mainly utilizes wet specimens that have been rehydrated. A few studies investigated bone utilizing dry specimens [126–130]. Bargen et al. [130], Carter et al. [126], and Samuel et al. [127] found that bone specimens that had been dried possessed increased stiffness in comparison with fresh bone specimens. Guillaume et al. [128] assessed dry, dried then rehydrated, and fresh thawed bone specimens and found that dried then rehydrated bone specimens exhibited properties closer to fresh thawed bone. This work, in contrast to the processes mentioned above, preserved the moisture of the bone by utilizing fresh thawed bone with no drying and rehydration process. This was done to ensure that the bone stayed as close to its natural state as possible for a more accurate depiction of the behaviour in-vivo. Moisture loss was minimized by wrapping the specimen in cling film when the specimen was not in use. Beyond moisture loss, the study of the contribution of anisotropy was avoided with these protocols.

Since anisotropy has been found to play a significant role in the mechanical behaviour of bone, this work ensured consistency in the fabrication process by the use of a custom

rig. This ensured that even if a degree change in alignment occurred, there would be consistency across all fabricated specimens. Without anisotropy managed, the analysis of mechanical properties could have been affected by the geometric properties of the specimens.

Intrinsic mechanical properties like Young's modulus have been proven to be affected by area and length [44,60]. Therefore, an analysis was conducted to evaluate whether any significant differences existed between the fabricated specimens. The analysis (results in section 6.1) showed that there was no significant difference between the dimensions of specimens utilized for compression and tension. This analysis was vital in order to allow valid comparison across specimen groups tested. Since the dimensions of the specimens were not significantly different from each other, the contribution of diameter and length were considered controlled. There was no need to include them in the analysis as confounding variables. Possible errors arising due to specimen's shape were minimized with the utilization of cylindrical specimens. This is in line with the recommendations of Linde et al. [44] and Keaveny et al. [56] who suggest that the utilization of cylindrical specimens with a diameter greater than 5mm while maintaining aspect ratio would minimize buckling.

The fabricated specimens were grouped into compression and tension with similar samples existing in each group. The densities of both groups were analyzed, and it was found that they were statistically not different from each other.

A comparison of the established ash density-mechanical property and density ratio-mechanical property relationships show that the density ratio showed better correlations with bone stiffness and strength than mineral density. The correlations are summarised in Table 23 and Table 24 below for easier reference.

Table 23: Summary of the outcomes of modulus-density variations under investigation.

Test Type	Bone Type	Power-Law Model			Linear Regression		
		$E{-}\rho_{ash}$ R²	$E-\rho_{ash}/\rho_{org}$ R²	$E{-}\rho_{org}$ R²	$E-\rho_{ash}$ R²	$E-\rho_{ash}/\rho_{org}$ R²	$E{-}\rho_{org}$ R²
Compres-sion	Pooled	0.784	**0.791**	0.540	0.874	**0.880**	0.550
	Cortical	**0.514**	0.502	0.004	0.469	**0.497**	0.033
	Cancellous	0.177	**0.197**	0.017	**0.162**	0.155	0.038
Tension	Pooled	0.775	**0.780**	0.497	**0.927**	0.923	0.498
	Cortical	0.242	**0.446**	0.002	0.255	**0.433**	0.005
	Cancellous	0.240	**0.273**	0.089	0.194	**0.207**	0.082

*Bolded R² values refer to the highest obtained for that tested group.

Table 24: Summary of the outcomes of peak stress-density variations under investigation.

Test Type	Bone Type	Power-Law Model		Linear Regression	
		$\sigma-\rho_{ash}$ R²	$\sigma-\rho_{ash}/\rho_{org}$ R²	$\sigma-\rho_{ash}$ R²	$\sigma-\rho_{ash}/\rho_{org}$ R²
Compression	Pooled	0.799	**0.851**	0.847	**0.864**
	Cortical	0.405	**0.539**	0.347	**0.455**
	Cancellous	0.347	**0.426**	0.333	**0.379**
Tension	Pooled	0.630	**0.634**	0.671	**0.689**
	Cortical	0.016	0.064	0.017	0.091
	Cancellous	0.207	**0.225**	0.502	**0.510**

* Bolded R² values refer to the highest obtained for that tested group.
** The cortical bone types were not bolded since their significance levels were $> p = 0.05$.

The utilization of organic content information alone for predicting bone behaviour yielded poor results – specifically in the cortical and cancellous bone cohorts – as expected since the structural behaviour of bone is dependent on mineral content. The pooled bones however, showed a positive correlation ($R = 0.74$, $R^2 = 0.55$) between compressive properties and organic density; and a positive correlation ($R = 0.71$, $R^2 = 0.50$) between tensile properties and organic density. This implies a 50% correlation between bone stiffness and

organic density. It is expected that the correlation between bone stiffness and organic density will be stronger if a better model is used. The power and linear model were used since these are predominant in bone research. Existing models only considered mineral density and so other models have not been explored. This finding cannot be understated because it suggests organic content plays a role in the description of bone strength. This could possibly a synergistic role with mineral density. The combination of both organic content and mineral content information yielded better results than that of just mineral content. The results should however be interpreted with caution as the density ratio utilized for this work is only one possible interaction that might exist between ash density and organic density. More work is needed to identify the mechanism of interaction between the two elements.

At this time, issues with low R^2 values may be attributed to methodological difficulties in testing of specific specimen groups. During testing, specific specimens needed to be retested as they yielded no data once testing had begun. The initial failed test most likely altered the behaviour of the specimen, and so uniformity in testing across specimens was not guaranteed. The justification for the inclusion of these data, however, is that since the software recorded no load readings for such specimens, the effect of the failed test is minimal. Some specimens were not appropriately inspected during the fabrication stage and were recognized as two bones stacked on each other. Such data were removed from the analyzed results. Another explanation for the variance in the tested data might be because the leg bones obtained were not distinguished from each other by the butcher and might be combinations of femur and tibia.

Despite these shortcomings, the results obtained in this study suggest that organic content plays a role in improving the accuracy of bone mechanical property prediction. This

finding is critical because loss of bone organic content has been linked with age [131]. This implies that existing relationships may need to include organic content in future relationships in order to protect the vulnerable aging population. The positive correlation-increase obtained from the utilization of organic-mineral relationships also indicates that organic content information cannot be overlooked.

Chapter 7

Conclusions and Future Work

7.1   Conclusions and Contributions

Existing studies on bone mechanical behaviour have been affected adversely by different parameters already introduced in this thesis. The organic content information, while noticeably necessary for defining the biomechanical properties exhibited by bone, has been left out in the development of macro-scale empirical relationships evaluating bone stiffness. Furthermore, the anisotropic nature of bone further complicates the study of bone and limits the tests significantly. This project aimed to investigate the effect of organic proteins and water on the mechanical properties of bone by developing a novel experimental protocol. The reason for prioritizing strict experimental protocols is to enable confidence in the utilization of data obtained from the outlined process (by managing anisotropy). Based on the research gaps, the significant contributions and conclusions of the present work are as follows:

- Anisotropy was managed by the development of a custom-rigged mould suitable for use on bovine leg bone regardless of size. The mould ensured consistency among each specimen fabricated from the whole bone in the longitudinal orientation. Furthermore, this technique is practical for use in the fabrication of large numbers of specimens. This approach for avoiding anisotropy is a novel contribution of this thesis to the existing body of work.

- The repeatability of manufacturing and testing specimens according to the procedures outlined is promising as samples produced and tested over several months of work are not significantly different from each other. This is significant because existing protocols were difficult to reproduce.

- Moisture loss was managed by leaving the specimen in cling film and freezing – in contrast with the majority of existing work, which prefers drying and rehydration. This approach ensured that bones were tested as close to physiologic conditions as possible without external intervention.

- A novel Ashing procedure was developed for the analysis of bone inorganic and organic compositions.

- In both compression and tension tests of pooled bones, organic density showed 50% correlation with bone stiffness ($R = 0.70$, $R^2 = 0.50$).

- The inclusion of organic content information with mineral content in description of bone behaviour yielded generally better R^2 values than those utilizing just mineral content information – suggesting that organic-mineral interaction plays a role in defining the mechanical properties of bone.

7.2   Limitations of the Present Study

Although the objectives of the work have been met, there exist a few limitations that can be associated with this study, as discussed below:

- This work was completed with an assumption that bone is uniform across each individual specimen. This means results obtained from this study need to be interpreted in the context of bone as a homogenous material. More work to examine the behavior of bone as a heterogenous material would need to be conducted as that was beyond the scope of this work.

- The degree of anisotropy was not quantified and examined as expensive equipment would have been required, and none was readily available. Quantifying the degree of anisotropy and grouping the specimens accordingly might lead to more accurate results.

- The accuracy of the density measurements obtained indirectly from weight measurement devices was questionable. Several measurements of the same material were tested and averaged; however, a more accurate weight scale should have been used.

- End-artifacts were not considered in the preparation of this protocol as platens (for compression), and grips (for tension) were utilized. Misalignment was avoided through manual processes and cannot be trusted in experiments testing many specimens.

- The displacements and strains were obtained from the movement of the crosshead and might be affected by machine compliance effects [91].

- The tissue behaviour equations utilized in this study relied on sets of empirically derived constants based on the dataset. Their applicability in the prediction of bone strength is thus unknown until an external validation study with an independent data set is conducted.

- The power law and linear models were utilized for modeling all relationships in this study. Better models will be able to show a stronger correlation between organic density and bone stiffness. The power and linear models were used since existing work utilizes those models. One possible reason other models were not explored in the literature is because the focus of existing work has been on mineral density.

- The study of the interaction between ash density and organic density was limited to the density ratio. The interaction however is a more complex mechanism that was beyond the scope of this work at this time.

While these limitations have been outlined, it is important to recognize the difficulty in controlling for every single source of error in such a large-scale work. The very nature of this project possesses some inherent limitations – like anisotropy control. To that end, this work focused on producing protocols in which accuracies (and inaccuracies) are consistent across implementation to allow for assessment of expected results.

7.3   Future Work

The potential benefits of useful data from an increasingly accurate empirical relationship between bone components and its mechanical properties are enormous. From osteoporosis

prediction improvement – to fracture risk improvement – to finite element modelling accuracy improvement, the possibilities for the future are endless. To achieve such long-term dreams, prospective future work should be first tailored to improving this protocol in these areas:

- The utilization of silicone material for the custom-rigged mould as opposed to the current wooden material. Silicone is biocompatible, cheaper in long-term use, and easier to manage.

- The utilization of optical measurements for collecting strain measurements in testing. The size of the samples constrains the use of extensometers in compression and some cases, tension.

- The utilization of the end-cap technique in tension testing might provide better accuracy and limit testing difficulties that arise from the gripping of the specimen.

The implementation of these recommendations may prove to be vital in this pivotal pilot work investigating bone composition on mechanical properties at the macro-scale with the inclusion of organic content. Additional future work that can be completed may thus include:

- Development and optimization of empirical relationships incorporating organic content information. These relationships would need to determine the exact mechanism of interaction between organic content and mineral content.

- Validation of these relationships against an independent data set, and the existing body of work.

- Studying the contribution of anisotropy with respect to the influence of organic-mineral composition on the mechanical properties of bone.

A successful outcome of these prospective studies would be beneficial for patients and clinicians in the next generation of health technology.

Bibliography

1.   Mirzaei M, Keshavarzian M, Naeini V. Analysis of strength and failure pattern of human proximal femur using quantitative computed tomography (QCT)-based finite element method. *Journal of Bone*. 64, 108–114 (2014).

2.   Barrett-Connor E. The economic and human costs of osteoporotic fracture. *American Journal of Medicine.* 98(2 SUPPL. 1), 3S–8S (1995).

3.   Gullberg B, Johnell O, Kanis JA. World-wide Projections for Hip Fracture. *Osteoporosis. International.* 7, 407–413 (1997).

4.   Pfeifer M, Minne HW. Musculoskeletal rehabilitation after hip fracture: a review. *Arch. Osteoporosis* 5(1–2), 49–59 (2010).

5.   Ballane G, Cauley JA, Arabi A, El-Hajj Fuleihan G. Chapter 27 – Geographic Variability in Hip and Vertebral Fractures. In: *Osteoporosis*. Marcus R, Feldman D, Dempster DW, Luckey M, Cauley J (Eds.). Elsevier, 623–644 (2013).

6.   Wolford ML, Palso K, Bercovitz A. Hospitalization for Total Hip Replacement Among Inpatients Aged 45 and Over: United States, 2000–2010 Key findings. Hyattsville.

7.   Amoako AO, Pujalte GGA. Osteoarthritis in young, active, and athletic individuals. *Clin. Med. Insights. Arthritis Musculoskelet. Disord.* 7, 27–32 (2014).

8.   Helgason B, Gilchrist S, Ariza O, *et al.* The influence of the modulus–density relationship and the material mapping method on the simulated mechanical response of the proximal femur in side-ways fall loading configuration. *Med. Eng. Phys.* 38(7), 679–689 (2016).

9.   Dong XN, Acuna RL, Luo Q, Wang X. Orientation dependence of progressive post-yield behavior of human cortical bone in compression. (2012).

10.   Ritchie RO, Koester KJ, Ionova S, Yao W, Lane NE, Ager JW. Measurement of the toughness of bone: A tutorial with special reference to small animal studies. *Bone*. 43(5), 798–812 (2008).

11.   Sandino C, Mcerlain DD, Schipilow J, Boyd SK. Mechanical stimuli of trabecular

bone in osteoporosis: A numerical simulation by finite element analysis of microarchitecture. *J. Mech. Behav. Biomed. Mater.* 66, 19–27 (2016).

12. Van Lenthe GH, Stauber M, Müller R. Specimen-specific beam models for fast and accurate prediction of human trabecular bone mechanical properties. *Bone.* 39(6), 1182–1189 (2006).

13. Doblar M, Garc Ia JM, Omez MJG. Modelling bone tissue fracture and healing: a review. *Eng. Fract. Mech.* 71, 1809–1840 (2004).

14. Helgason B, Taddei F, Pálsson H, *et al.* A modified method for assigning material properties to FE models of bones. *Med. Eng. Phys.* 30, 444–453 (2008).

15. Zhao S, Arnold M, Ma S, *et al.* Standardizing Compression Testing for Measuring the Stiffness of Human Bone. *Bone Jt. Res.* 7(8), 524–538 (2018).

16. Kopperdahl DL, Keaveny TM. Yield strain behavior of trabecular bone. *Journal of. Biomechanics.* 31(7), 601–608 (1998).

17. Öhman C, Baleani M, Perilli E, *et al.* Mechanical testing of cancellous bone from the femoral head: Experimental errors due to off-axis measurements. *Journal of Biomechanics.* 40(11), 2426–2433 (2007).

18. Zapata-Cornelio FY, Day GA, Coe RH, *et al.* Methodology to Produce Specimen-Specific Models of Vertebrae: Application to Different Species. *Ann. Biomed. Eng.* 45(10), 2451–2460 (2017).

19. Carpenter RD. Finite Element Analysis of the Hip and Spine Based on Quantitative Computed Tomography. *Curr. Osteoporos. Rep.* 11(2), 156–162 (2013).

20. Engelke K, Libanati C, Fuerst T, Zysset P, Genant HK. Advanced CT based In Vivo Methods for the Assessment of Bone Density, Structure, and Strength. *Curr. Osteoporos. Rep.* 11(3), 246–255 (2013).

21. Gomes EA, Diana HH, Oliveira JS, *et al.* Reliability of FEA on the Results of Mechanical Properties of Materials. *Braz. Dent. J.* 26(6), 667–670 (2015).

22. Veríssimo C, Simamoto Júnior PC, Soares CJ, Noritomi PY, Santos-Filho PCF. Effect of the crown, post, and remaining coronal dentin on the biomechanical behavior of endodontically treated maxillary central incisors. *J. Prosthet. Dent.* 111(3), 234–246 (2014).

23. Luo Y. Image-Based Multilevel Biomechanical Modeling for Fall-Induced Hip Fracture. Springer Nature.

24. Wirtz DC, Schiffers N, Pandorf T, Radermacher K, Weichert D, Forst R. Critical evaluation of known bone material properties to realize anisotropic FE-simulation of the proximal femur. *Journal of Biomechanics.* 33, 1325–1330 (2000).

25. Carter DR, Hayes WC. The Compressive Behavior Porous of Bone Structure as a Two-Phase. *J. bone Jt. Surg.* 59(7), 954–962 (1977).

26. Currey JD. The effect of porosity and mineral content on the Young's modulus of elasticity of compact bone. *J. Biomech.* 21(2), 131–139 (1988).

27. Keller TS. Predicting the Compressive Mechanical Behavior of Bone*. *Journal of Biomechanics.* 27(9), 1159–1168 (1994).

28. Rice JC, Cowin SC, Bowman JA. On the dependence of the elasticity and strength of cancellous bone on apparent density. *J. Biomech.* 21(2), 155–168 (1988).

29. Nicholson PHF, Cheng XG, Lowet G, *et al.* Structural and material mechanical properties of human vertebral cancellous bone. *Med. Eng. Phys.* 19(8), 729–737 (1997).

30. Hodgskinson R, Currey JD. Young's modulus, density and material properties in cancellous bone over a large density range. *J. Mater. Sci. Mater. Med.* 3(5), 377–381 (1992).

31. Rho JY, Ashman RB, Turner CH. Young's modulus of trabecular and cortical bone material: Ultrasonic and microtensile measurements. *J. Biomech.* 26(2), 111–119 (1993).

32. Burgers TA, Mason J, Niebur G, Ploeg HL. Compressive properties of trabecular bone in the distal femur. *J. Biomech.* 41(5), 1077–1085 (2008).

33. Lotz JC, Gerhart TN, Hayes WC. Mechanical Properties of Metaphyseal Bone in the Proximal Femur. *J. Biomech.* 24(5), 317–329 (1991).

34. Snyder SM, Schneider E. Estimation of mechanical properties of cortical bone by computed tomography. *J. Orthop. Res.* 9(3), 422–431 (1991).

35. Rho JY, Hobatho MC, Ashman RB. Relations of mechanical properties to density and CT numbers in human bone. *Med. Eng. Phys.* 175(17), 347–355 (1995).

36. Bernard S, Schneider J, Varga P, Laugier P, Raum K, Grimal Q. Elasticity–density and viscoelasticity–density relationships at the tibia mid-diaphysis assessed from resonant ultrasound spectroscopy measurements. *Biomech. Model. Mechanobiol.* 15(1), 97–109 (2016).

37. Hengsberger S, Enstroem J, Peyrin F, Zysset P. How is the indentation modulus of bone tissue related to its macroscopic elastic response? A validation study. *J. Biomech.* 36, 1503–1509 (2003).

38. Mirzaali MJ, Schwiedrzik JJ, Thaiwichai S, *et al.* Mechanical properties of cortical bone and their relationships with age, gender, composition and microindentation properties in the elderly. (2016).

39. Helgason B, Perilli E, Schileo E, Taddei F, Brynjólfsson S, Viceconti M. Mathematical relationships between bone density and mechanical properties: A literature review. *Clin. Biomech.* 23(2), 135–146 (2008).

40. Wille H, Rank E, Yosibash Z. Prediction of the mechanical response of the femur with uncertain elastic properties. *J. Biomech.* 45, 1140–1148 (2012).

41. Carter DR, Hayes WC. Bone Compressive Strength: The Influence of Density and Strain Rate. *Am. Assoc. Adv. Sci.* 194(4270), 1174–1176 (1976).

42. Sievänen H, Kannus P, Nieminen V, Heinonen A, Oja P, Vuori I. Estimation of various mechanical characteristics of human bones during dual energy x-ray absorptiometry: methodology and precision. *Bone.* 18(1), S17–S27 (1996).

43. Ciarelli MJ, Goldstein SA, Kuhn JL, Cody DD, Brown MB. Evaluation of orthogonal mechanical properties and density of human trabecular bone from the major metaphyseal regions with materials testing and computed tomography. *J. Orthop. Res.* 9(5), 674–682 (1991).

44. Linde F, Hvid I, Madsen F. The Effect of Specimen Geometry on the Mechanical Behaviour of Trabecular Bone Specimen. *J. Biomech.* 25(4), 359–368 (1992).

45. Keyak JH, Lee IY, Skinner HB. Correlations between orthogonal mechanical properties and density of trabecular bone: Use of different densitometric measures. *J. Biomed. Mater. Res.* 28(11), 1329–1336 (1994).

46. Goulet RW, Goldstein SA, Ciarelli MJ, Kuhn JL, Brownt MB, Feldkamp LA. The relationship between the structural and orthogonal compressive properties of trabecular bone. *Journal of Biomechanics.* 21(4), 375–389 (1994).

47. Ciarelli TE, Fyhrie DP, Schaffler MB, Goldstein SA. Variations in Three-Dimensional Cancellous Bone Architecture of the Proximal Femur in Female Hip Fractures and in Controls. *J. Bone Miner. Res.* 15(1), 32–40 (2000).

48. Cory E, Nazarian A, Entezari V, Vartanians V, Müller R, Snyder BD. Compressive

axial mechanical properties of rat bone as functions of bone volume fraction, apparent density and micro-ct based mineral density. *J. Biomech.* 43(5), 953–960 (2010).

49.   Hansson TH, Keller TS, Panjabi MM. A study of the compressive properties of lumbar vertebral trabeculae: Effects of tissue characteristics. *Spine (Phila. Pa. 1976).* 12(1), 56–62 (1987).

50.   Mosekilde L, Mosekilde L, Danielsen CC, Mosekilde L. Biomechanical Competence of Vertebral Trabecular Bone in Relation to Ash Density and Age in Normal Individuals. *Bone.* 8(2), 79–85 (1987).

51.   Nobakhti S, Shefelbine SJ. On the Relation of Bone Mineral Density and the Elastic Modulus in Healthy and Pathologic Bone. *Curr. Osteoporos. Rep.* 16, 404–410 (2018).

52.   Martin RB, Boardman DL. The effects of collagen fiber orientation, porosity, density, and mineralization on bovine cortical bone bending properties. *J. Biomech.* 26(9), 1047–1054 (1993).

53.   Schaffler MB, Burr DB. Stiffness of compact bone: Effects of porosity and density. *J. Biomech.* 21(1), 13–16 (1988).

54.   Banse X, Sims TJ, Bailey AJ. Mechanical Properties of Adult Vertebral Cancellous Bone: Correlation With Collagen Intermolecular Cross-Links. *J. Bone Miner. Res.* 17(9), 1621–1628 (2002).

55.   Linde F, Christian H, Sorensen F. The Effect of Different Storage Methods on the Mechanical Properties of Trabecular Bone. *J. Biomech.* 26(10), 1249–1252 (1993).

56.   Keaveny TM, Pinilla TP, Crawford RP, Kopperdahl DL, Lou A. Systematic and Random Errors in Compression Testing of Trabecular Bone. *J. Orthop. Res.* 15(1), 101–110 (1997).

57.   Wen X-X, Xu C, Zong C-L, *et al.* Relationship between sample volumes and modulus of human vertebral trabecular bone in micro-finite element analysis. *J. Mech. Behav. Biomed. Mater.* 60, 468–475 (2016).

58.   Ün K, Bevill G, Keaveny TM. The effects of side-artifacts on the elastic modulus of trabecular bone. *J. Biomech.* 39(11), 1955–1963 (2006).

59.   Morgan EF, Keaveny TM. Dependence of yield strain of human trabecular bone on anatomic site. *J. Biomech.* 34(5), 569–577 (2001).

60.   Zhu M, Keller TS, Spengler DM. Effects of specimen load-bearing and free surface

layers on the compressive mechanical properties of cellular materials. *J. Biomech.* 27(1), 57–66 (1994).

61.   Linde F, Gøosthgen CB, Hvid I, Pongsoipetch B, Bentzen S. Mechanical Properties of Trabecular Bone by a Non-Destructive Compression Testing Approach. *Eng. Med.* 17(1), 23–29 (1988).

62.   Keaveny TM, Guo XE, Wachtel EF, Mcmahont TA, Hayes WC. Trabecular Bone Exhibits Fully Linear Elastic Beahavior and Yields at Low Strains. *J. Biomech.* 27(9), 1127–1136 (1994).

63.   Keaveny TM, Borchers RE, Gibson LJ, Hayes WC. Theoretical analysis of the experimental artifact in trabecular bone compressive modulus. *J. Biomech.* 26(4–5), 599–607 (1993).

64.   Odgaard A, Linde F. The Underestimation of Young's Modulus in Compressive Testing of Cancellous Bone Specimens. *J. Biomech.* 24(8), 691–698 (1991).

65.   Schett G. Biology, Physiology, and Morphology of Bone. Tenth Edit. Elsevier Inc.

66.   Weiner S, Wagner HD. THE MATERIAL BONE: Structure-Mechanical Function Relations. *Annu. Rev. Mater. Sci.* 28, 271–298 (1998).

67.   Pepper M, Akuthota V, Mccarty EC. The Pathophysiology of Stress Fractures. *Clin. Sports Med.* 25(1), 1–16 (2005).

68.   Olszta MJ, Cheng X, Jee SS, *et al.* Bone structure and formation: A new perspective. *Mater. Sci. Eng. Reports.* 58(3–5), 77–116 (2007).

69.   Thurner PJ, Lam S, Weaver JC, Morse DE, Hansma PK. Localization of Phosphorylated Serine, Osteopontin, and Bone Sialoprotein on Bone Fracture Surfaces. *J. Adhes.* 85(8), 526–545 (2009).

70.   Sasaki N, Matsushima N, Ikawa T, Yamamura H, Fukuda A. Orientation of Bone Mineral and its Role in the Anisotropic Mechanical Properties of Bone - Transverse Anisotropy. *J. Biomech.* 22(2), 157–164 (1989).

71.   Novitskaya E, Chen PY, Lee S, *et al.* Anisotropy in the compressive mechanical properties of bovine cortical bone and the mineral and protein constituents. *Acta Biomater.* 7(8), 3170–3177 (2011).

72.   Currey JD. Role of collagen and other organics in the mechanical properties of bone. *Osteoporos. Int.* 14(0), 29–36 (2003).

73.   Currey JD, Zioupos P, Davies P, Casinos A. Mechanical properties of nacre and

highly mineralized bone. *Proc. R. Soc. B Biol. Sci.* 268(1462), 107–111 (2001).

74. Fung A. Experimental Validation of Finite Element Predicted Bone Strain in the Human Metatarsal. (2017).

75. Currey JD. Bones: Structure and Mechanics. Princeton University Press, Princeton, N.J.

76. Manilay Z, Novitskaya E, Sadovnikov E, Mckittrick J. A comparative study of young and mature bovine cortical bone. *Acta Biomater.* 9(2), 5280–5288 (2013).

77. Santiuste C, Rodríguez-Millán M, Giner E, Miguélez H. The influence of anisotropy in numerical modeling of orthogonal cutting of cortical bone. *Compos. Struct.* 116, 423–431 (2014).

78. Bonfield W, Grynpas MD. Anisotropy of the Young's modulus of bone. *Nature.* 270(December 15), 453 (1977).

79. Reilly DT, Burstein AH. The Elastic and Ultimate Properties of Compact Bone Tissue. *J. Biomech.* 8(6), 393–405 (1975).

80. Li S, Demirci E, Silberschmidt V V. Variability and anisotropy of mechanical behavior of cortical bone in tension and compression. *J. Mech. Behav. Biomed. Mater.* 21, 109–120 (2013).

81. Hasegawa K, Turner CH, Burr DB. Contribution of Collagen and Mineral to the Elastic Anisotropy of Bone. *Calcif. Tissue Int.* 55(5), 381–386 (1994).

82. Iyo T, Maki Y, Sasaki N, Nakata M. Anisotropic viscoelastic properties of cortical bone. *J. Biomech.* 37(9), 1433–1437 (2004).

83. Novitskaya E, Chen P-Y, Lee S, *et al.* Anisotropy in the compressive mechanical properties of bovine cortical bone and the mineral and protein constituents. *Acta Biomater.* 7, 3170–3177 (2011).

84. Szabó ME, Thurner PJ. Anisotropy of bovine cortical bone tissue damage properties. *J. Biomech.* 46, 2–6 (2012).

85. Lotz JC, Gerhart TN, Hayes WC. Mechanical Properties of Trabecular Bone from the Proximal Femur: A Quantitative CT Study. *J. Comput. Assist. Tomogr.* 14(1), 107–114 (1990).

86. Bourgnon A, Sitzer A, Chabraborty A, *et al.* Impact of Microscale Properties Measured by 50-MHz Acoustic Microscopy on Mesoscale Elastic and Ultimate Mechanical Cortical Bone Properties. In: *2014 IEEE International Ultrasonics Symposium.*

IEEE, Chicago, IL, USA, 636–638 (2014).

87.   Zhou B, Sherry Liu X, Wang J, Lucas Lu X, Fields AJ, Edward Guo X. Dependence of mechanical properties of trabecular bone on plate-rod microstructure determined by individual trabecula segmentation (ITS). *J. Biomech.* 47(3), 702–708 (2014).

88.   Majumdar S, Lin J, Link T, *et al.* Fractal analysis of radiographs: Assessment of trabecular bone structure and prediction of elastic modulus and strength. *Med. Phys.* 26(7), 1330–1340 (1999).

89.   Schwiedrzik J, Gross T, Bina M, Pretterklieber M, Zysset P, Pahr D. Experimental validation of a nonlinear μFE model based on cohesive-frictional plasticity for trabecular bone. *Int. j. numer. method. biomed. eng.* 32(4) (2016).

90.   Lv H, Zhang L, Yang F, *et al.* Comparison of microstructural and mechanical properties of trabeculae in femoral head from osteoporosis patients with and without cartilage lesions: A case-control study Pathophysiology of musculoskeletal disorders. *BMC Musculoskelet. Disord.* 16(1), 1–10 (2015).

91.   Zhao S, Arnold M, Ma S, *et al.* Standardizing compression testing for measuring the stiffness of human bone. *Bone Joint Res.* 7(8), 524–538 (2018).

92.   Boskey AL, Coleman R. Aging and Bone. *J Dent Res*. 89(12), 1333–1348 (2010).

93.   Knott L, Bailey AJ, Knott L. Collagen Cross-Links in Mineralizing Tissues: A Review of Their Chemistry, Function, and Clinical Relevance. *Bone*. 22(3), 181–187 (1998).

94.   Wang X. Cortical Bone Mechanics and Composition: Effects of Age and Gender. Springer US.

95.   Maquer G, Musy SN, Wandel J, Gross T, Zysset PK. Bone Volume Fraction and Fabric Anisotropy Are Better Determinants of Trabecular Bone Stiffness Than Other Morphological Variables. *J. Bone Miner. Res.* 30(6), 1000–1008 (2015).

96.   Musy SN, Maquer G, Panyasantisuk J, Wandel J, Zysset PK. Not only stiffness, but also yield strength of the trabecular structure determined by non-linear ï¿½FE is best predicted by bone volume fraction and fabric tensor. *J. Mech. Behav. Biomed. Mater.* 65 (2017).

97.   Dalstra M, Huiskes ~ R, Odgaard~ $ A, Van Erning L. Mechanical and Textural Properties of Pelvic Trabecular Bone*. *J. Biomech.* 26(4/5), 523–535 (1993).

98.   Grynpas MD, Tupy JH, Sodek J. The distribution of soluble, mineral-bound, and

matrix-bound proteins in osteoporotic and normal bones. *Bone*. 15(5), 505–513 (1994).

99. Chen P-Y, McKittrick J. Compressive mechanical properties of demineralized and deproteinized cancellous bone. *J. Mech. Behav. Biomed. Mater.* 4(7), 961–973 (2011).

100. Hansen U, Zioupos P, Simpson R, Currey JD, Hynd D. The Effect of Strain Rate on the Mechanical Properties of Human Cortical Bone. *J. Biomech. Eng.* 130(1), 011011 (2008).

101. Bevill G, Eswaran SK, Farahmand F, Keaveny TM. The influence of boundary conditions and loading mode on high-resolution finite element-computed trabecular tissue properties. *Bone*. 44, 573–578 (2008).

102. Linde F, Sørensen HCF. The effect of different storage methods on the mechanical properties of trabecular bone. *J. Biomech.* 26(10), 1249–1252 (1993).

103. Morgan EF, Yeh OC, Chang WC, Keaveny TM. Nonlinear Behavior of Trabecular Bone at Small Strains. *J. Biomech. Eng.* 123(1), 1 (2001).

104. Zhu M, Keller TS, Spengler DM. Effects of Specimen Load-Bearing and Free Surface Layers on the Compressive Mechanical Properties of Cellular Materials. *J. Biomech.* 27(I), 57–66 (1994).

105. Ouyang' J, Yang GT, Wu2 WZ, Zhul QA, Zhongl SZ. Biomechanical characteristics of human trabecular bone.

106. Keaveny TM, Wachtel EF, Ford CM, Hayes WC. Differences Between the Tensile and Compressive Strengths of Bovine Tibial Trabecular Bone depend on Modulus. *J. Biomech.* 27(9), 1137–1146 (1994).

107. Keaveny TM, Borchers RE, Gibson~ LJ, Hayes WC. Trabecular Bone Modulus and Strength can Depend on Specimen Geometry. *J. Biomech.* 26(8), 991–1000 (1993).

108. Gibson LJ. The Mechanical Behavior of Cancellous Bone. *J. Biomech.* 18(5), 317–328 (1985).

109. Lievers WB, Waldman SD, Pilkey AK. Minimizing specimen length in elastic testing of end-constrained cancellous bone. *J. Mech. Behav. Biomed. Mater.* 3(1), 22–30 (2010).

110. An YH, Draughn RA. Mechanical Testing of Bone and the Bone-Implant Interface. CRC Press (2002).

111. Aspden RM. Mechanical Testing of Bone Ex Vivo. In: *Bone Research Protocols*. Helfrich MH, Ralston SH (Eds.). . Humana Press, New Jersey, 369–380 (2003).

112. Jepsen Laboratory. Bone harvesting protocol. Ann Arbor.

113. Public Agency of Canada. Canadian Biosafety Standard. Ottawa.

114. Högset O, Bredberg G. Plaster of Paris: Thermal Properties and Biocompatibility. *Acta Otolaryngol.* 101(5–6), 445–456 (2009).

115. ASTM International. ASTM E111-17 Standard Test Method for Young's Modulus, Tangent Modulus, and Chord Modulus. West Conshohocken, PA.

116. ASTM International. E4 − 16 Standard Practices for Force Verification of Testing Machines. (2016).

117. ASTM International. D638-14 Standard Test Method for Tensile Properties of Plastics. (2014).

118. ASTM International. E8/E8M-16a Standard Test Methods for Tension Testing of Metallic Materials. (2016).

119. ASTM International. D882-18 Standard Test Method for Tensile Properties of Thin Plastic Sheeting. (2018).

120. ASTM International. D3574-17 Standard Test Methods for Flexible Cellular Materials - Slab, Bonded, and Molded Urethane Foams. (2017).

121. ASTM International. D412-16 Standard Test Methods for Vulcanized Rubber and Thermoplastic Elastomers - Tension. (2016).

122. Jepsen Laboratory. Ash Content Protocol. Ann Arbor.

123. Morgan EF, Bayraktar HH, Keaveny TM. Trabecular bone modulus–density relationships depend on anatomic site. *J. Biomech.* 36(7), 897–904 (2003).

124. Li B, Aspden RM. Composition and Mechanical Properties of Cancellous Bone from the Femoral Head of Patients with Osteoporosis or Osteoarthritis. *J. Bone Miner. Res.* 12(4), 641–651 (1997).

125. Kaneko TS, Bell JS, Pejcic MR, Tehranzadeh J, Keyak JH. Mechanical properties, density and quantitative CT scan data of trabecular bone with and without metastases. *J. Biomech.* 37(4), 523–530 (2004).

126. Carter DR, Schwab GH, Spengler DM. Tensile fracture of cancellous bone. *Acta Orthop.* 51(1–6), 733–741 (1980).

127. Samuel J, Park J-S, Almer J, Wang X. Effect of water on nanomechanics of bone is different between tension and compression. *J. Mech. Behav. Biomed. Mater.* 57, 128–138 (2016).

128. Erivan R, Villatte G, Cueff R, Boisgard S, Descamps S. Rehydration improves the ductility of dry bone allografts. *Cell Tissue Bank.* 18(3), 307–312 (2017).

129. Pothuaud L, Van Rietbergen B, Mosekilde L, *et al.* Combination of topological parameters and bone volume fraction better predicts the mechanical properties of trabecular bone. *Journal of Biomechanics.* 35, 1091–1099 (2002).

130. Bargren JH, Bassett CAC, Gjelsvik A. Mechanical Properties of Hydrated Cortical Bone*. *J. Biomech.* 7(3), 239–242 (1974).

131. Boskey AL, Imbert L. Bone quality changes associated with aging and disease: a review. *Ann. N. Y. Acad. Sci.* 1410(1), 93–106 (2017).

132. Amromanoh O., Luo Y., Wu X. Experimental Study of the Effect of Organic and Mineral Content on Bone Mechanical Properties. *Joint congress of the Canadian Society for Mechanical Engineering and CFD Society of Canada Proceedings.* (2019).

133. Luo Y, Amromanoh O. An Inverse Study of Bone as an Organic-Inorganic Composite Material – Part A. *Journal of Biomedical Materials Research* (Under review).

Appendices

Appendix A

Sample Testing Form for Collecting Bone Information Prior-To, During, and Post-Test

MEASUREMENTS   mm   mm

Sample ID	MTS Labels	Weight (g)	Bone Type	L1	L2	D1	D2	AvgLength	AvgDiameter	Comments

ASHING

Sample ID	MTS Labels	Cup #	Weight (Cup + Samp)	Total Weight (with ash)	Weight (Empty Cup)
		1			
		2			

Testing Temperature	700C
Test Time	20 hours
Start Time	
Reached 700C	
End Time	

Appendix B

Testing The Furnace

We hypothesized that the initial problem with our programming of the furnace was a combination of inaccurate ramp rate and the short period of dwell time. Thermolyne technicians contacted us with more data to help clarify two things: how the dwell time affects the operation of the furnace and if the furnace is affected by the product load. The test data show that an empty furnace went from ambient temperature, T_{amb} (23°C) to maximum temperature, T_{max} (1200°C) in 80mins. This was used to obtain a starting point for the ramp rate (SP.RAT) to be tested. The assumption behind this was that the SP.RAT that would take the ambient temperature to the maximum temperature must have been the maximum capacity of the ramping of the furnace. This temperature could be wrong; hence, it was used as an initial starting point to test the device.

Since the SP.RAT is essentially the temperature (degrees Celsius) per minute that the furnace should try to reach the setpoint, the SP.RAT to reach T_{max} was

$$SP.RAT_{tmax} = \frac{T_{max} - T_{amb}}{Elapsed\ time} = \frac{1200°C - 23°C}{80mins} = 14.7$$

However, the SP.RAT to reach 300°C from their tests was calculated to be 27.7 (T_{amb} = 23°C, elapsed time = 10mins).

Testing Conditions:

Temperature: 500°C

Dwell time: 2 hours

Initial test SP.RAT was started at 30 and stepped down to 15 in intervals of 5 to evaluate performance.

Results:

- The dwell timer started at a temperature of 465°C.
- But the furnace took 26 mins to get to 500°C.
- The furnace turned off power output at 1hour 55mins.

Using a time of 26mins and following the above calculations,

the ramp rate was then set to 20. 20 is realistic since 15 (for max temperature) is less.

- The dwell timer started at a temperature of 490°C (sensible because our set threshold for countdown to begin was 10).
- The furnace turned off power output at precisely 2 hours.

Conclusions:

- The higher temperature and longer dwell time allow for what we program to show concrete results.
- A preliminary test for the realistic SP.RAT using the AUTOTUNE feature of the furnace would allow us to determine the SP.RAT for 650°C before we begin ashing testing.
  The operation of the furnace has been understood by Xinyi and I and testing can begin.